Published in final edited form as:

Plant J. 2019 May ; 98(3): 492–510. doi:10.1111/tpj.14232.

Chemical genetic identification of a lectin receptor kinase that transduces immune responses and interferes with abscisic acid signaling

Jiyoung Park[1], **Tae-Houn Kim**[2], **Yohei Takahashi**[1], **Rebecca Schwab**[3], **Keini Dressano**[1], **Aaron B Stephan**[1], **Paulo HO Ceciliato**[1], **Eduardo Ramirez**[1], **Vince Garin**[1], **Alisa Huffaker**[1], and **Julian I Schroeder**[1,*]

[1]Division of Biological Sciences, University of California, San Diego, 9500 Gilman Dr., La Jolla CA 92093-0116, USA

[2]Department of Biotechnology, Duksung Women's University, 01369, Seoul, Korea

[3]Department of Molecular Biology, Max Planck Institute for Developmental Biology, 72076 Tübingen, Germany

Abstract

Insight into how plants simultaneously cope with multiple stresses, for example, when challenged with biotic stress from pathogen infection and abiotic stress from drought, is important both for understanding evolutionary trade-offs and optimizing crop responses to these stresses. Mechanisms by which initial plant immune signaling antagonizes abscisic acid (ABA) signal transduction requires further investigation. Using a chemical genetics approach, the small molecule [5-(3,4-dichlorophenyl)furan-2-yl]-piperidine-1-ylmethanethione (DFPM) has previously been identified due to its ability to suppress ABA signaling via plant immune signaling components. Here, we have used forward chemical genetics screening to identify DFPM-insensitive loci by monitoring the activity of ABA-inducible *pRAB18::GFP* in the presence of DFPM and ABA. The ability of DFPM to attenuate ABA signaling was reduced in *rda* mutants (***r***esistant to ***D***FPM inhibition of ***A***BA signaling). One of the mutants, *rda2*, was mapped and is defective in a gene encoding a lectin receptor kinase. *RDA2* functions in DFPM-mediated inhibition of ABA-mediated reporter expression. *RDA2* is required for DFPM-mediated activation of immune signaling including phosphorylation of MAP kinase 3 (MPK3) and MPK6 and induction of immunity marker genes. Our study identifies a previously uncharacterized receptor kinase gene that is important for DFPM-mediated immune signaling and inhibition of abscisic acid signaling. We demonstrate that the lectin receptor kinase RDA2 is essential for perceiving the DFPM signal and activating MAP kinases, and that MKK4 and MKK5 are required for DFPM interference with ABA signal transduction.

Significance Statement

*For correspondence (jischroeder@ucsd.edu).

Conflict of interest

The authors declare no conflict of interest.

By activating plant immune signaling, the synthetic small molecule [5-(3,4-dichlorophenyl)furan-2-yl]-piperidine-1-ylmethanethione (DFPM) inhibits signaling by the drought-response hormone abscisic acid (ABA). DFPM thus provides a powerful tool for dissecting mechanisms that enable initial biotic signals to interfere with ABA signal transduction. We have used DFPM to identify, by a forward chemical genetics screen, a lectin receptor kinase that is essential to this process.

Keywords

Abscisic acid; cross-interference; lectin receptor kinase; DFPM; chemical genetics; plant defense; immune signaling; MAPK; *Arabidopsis thaliana*

Introduction

Plants are continuously challenged with environmental stresses that result in significant impact on plant growth and crop yields. Plants have evolved sophisticated stress tolerance mechanisms to minimize damage and to conserve resources for growth and reproduction. To investigate mechanisms of stress tolerance in plants, traditional research has focused on single stress conditions, for example by imposing individual stresses (Mittler et al., 2010). However, when plants face more than one stress simultaneously, their responses are not easily predictable based on responses to single stresses (Fujita et al., 2006, Atkinson et al., 2012, Ramegowda et al., 2015). Different pairs of environmental stresses result in different physiological and molecular responses, suggesting that plants utilize specific tolerance mechanisms depending on different stress combinations, which cannot be directly inferred from individual stress studies (Mittler et al., 2010, Suzuki et al., 2014). Therefore, detailed investigation of stress tolerance signaling pathways in defined combinations of stresses will be required.

Drought and pathogen infections are two major types of stresses that result in significant reduction in plant growth and yield (Wang et al., 2003, Bruce, 2010, Maxmen, 2013, Hatfield et al., 2015). Agricultural production will increasingly suffer from abiotic stresses including drought (Melillo et al., 2014) and biotic stresses (Oerke, 2005, Fischer et al., 2009). When plants are exposed to drought and pathogens at the same time, overall plant resistance is more reduced than by single stress conditions (Suzuki et al., 2014, Deutsch et al., 2018) and tolerance mechanisms against the two stresses often negatively regulate each other (Mauch-Mani et al., 2005, Prasch et al., 2013).

The phytohormone abscisic acid (ABA) is a major stress hormone that regulates plant responses to abiotic stresses including drought (Cutler et al., 2010, Finkelstein, 2013, Hauser et al., 2017). Roles of ABA and components of ABA signal transduction on regulating plant defense signaling have been discovered (Mauch-Mani et al., 2005, Yasuda et al., 2008, Ton et al., 2009, Bostock et al., 2014). ABA treatment increases pathogen susceptibility (Audenaert et al., 2002, Mohr et al., 2003, Asselbergh et al., 2008a, Fan et al., 2009, Ulferts et al., 2015, Buhrow et al., 2016). Negative roles of ABA in pathogen defense were also suggested by Arabidopsis and tomato mutants deficient in ABA synthesis (Asselbergh et al.,

2008a, Fan et al., 2009). Abiotic stress signaling pathways often act antagonistically on pathogen defense signaling under combinations of stresses (Asselbergh et al., 2008b).

Conversely, pathogen infections of plants often result in increased susceptibility to drought (Olson et al., 1990, Atkinson et al., 2015) and reduced responsiveness to ABA (Kim et al., 2011). Plants with increased levels of salicylic acid (SA), an important hormone for plant innate immunity and systemic acquired resistance (SAR), exhibited decreased drought resistance and ABA signal transduction (Németh et al., 2002, Yasuda et al., 2008, Mosher et al., 2010). However, other reports suggest that SA signaling enhances ABA signaling (Hayat et al., 2010, Khan et al., 2015). Therefore, this antagonistic interaction remains very complex and the underlying molecular mechanisms by which immune signaling pathways can interfere with ABA signal transduction remain largely elusive (Atkinson et al., 2015). Since pathogen infections induce complex, layered signaling pathways in plants depending on the pathogen species and time after infection (Fujita et al., 2006), imitating natural conditions to investigate interactions of tolerance mechanisms under drought and pathogen infection events has been difficult.

Chemical genetics is a powerful approach for dissecting signal transduction pathways through bypassing genetic redundancy, mutant lethality and network robustness (Park et al., 2009, Toth et al., 2010). The small molecule DFPM ([5-(3,4-dichlorophenyl)furan-2-yl]-piperidine-1-ylmethanethione) was isolated in a chemical genetics screen and interferes with ABA signal transduction by activating immune signaling (Kim et al., 2011). DFPM rapidly represses ABA-mediated gene expression, activation of slow-type anion channels, and ABA-induced stomatal closing (Kim et al., 2011). Early ABA signaling, including the interaction between the ABA receptor PYRABACTIN RESISTANCE1 (PYR1) and the protein phosphatase type 2C (PP2C) ABA INSENSITIVE1 (ABI1), and ABA-dependent activation of the protein kinase OPEN STOMATA1 (OST1), was not affected by DFPM (Kim et al., 2011). DFPM requires core components of effector-triggered immunity including *EDS1* and *PAD4* (Bhattacharjee et al., 2011, Heidrich et al., 2011) for DFPM-mediated inhibition of ABA signal transduction (Kim et al., 2011) and for an effector-triggered immune signaling components-requiring growth arrest response that is specific to roots (Kim et al., 2012, Kunz et al., 2016). The co-chaperons *RAR1* and *SGT1b* are also important for DFPM-mediated ABA interference signaling (Kim et al., 2011, Kim et al., 2012). Moreover, a Toll-Interleukin1 Receptor–nucleotide binding–Leucine-rich repeat (TIR-NB-LRR) protein VICTR is essential for DFPM-mediated root growth arrest (Kim et al., 2012, Kunz et al., 2016). Studies using DFPM provide evidence for a ‘cross-interference’ signal, which occurs from biotic stress signaling to inhibit ABA signal transduction and a platform to further dissect the molecular mechanisms for biotic-to-abscisic acid interference signaling.

Here we performed a forward genetic screen to find mutants with reduced levels of ABA signal transduction interference in response to DFPM. ***r****esistant to* ***D****FPM-inhibition of* ***A****BA signaling* (*rda*) mutant plants showing decreased sensitivity to DFPM in inhibiting ABA reporter expression were isolated. We mapped one of the *rda* mutants, *rda2*, to a previously uncharacterized lectin receptor-like kinase. RDA2 plays an important role in activating immune signaling and inhibits ABA signal transduction. RDA2 is required for perceiving a signal derived from DFPM and subsequently transducing immune signaling. Furthermore,

components of MAPK cascades including MAP kinase kinase 4 (MKK4) and MKK5 are involved in DFPM-mediated interference signaling.

Results

Chemical genetic screening for DFPM hypo-sensitive mutants

The small molecule DFPM ([5-(3,4-dichlorophenyl)furan-2-yl]- piperidine-1-ylmethanethione) was identified through its ability to rapidly inhibit ABA signal transduction by activating an immune signaling pathway (Kim et al., 2011). To dissect DFPM-mediated ABA interference signaling and to find genetic elements involved in this interference signaling, a forward-genetic screen was performed using DFPM (Figure S1). Columbia-0 (Col-0; wild-type) *Arabidopsis* seeds expressing the ABA response reporter *pRAB18::GFP* (Kim et al., 2011) were mutagenized with 1.5 to 3 % ethyl methanesulfonate (EMS). Two to three week-old M2 EMS mutant plants were exogenously treated with ABA and DFPM in which ABA-mediated induction of *pRAB18::GFP* fluorescence signal was inhibited in wild-type plants (Figure S1). Over 26,000 M2 lines were screened to isolate mutant plants which showed an ABA-induced *pRAB18::GFP* fluorescence signal in leaves despite treatment with 10 μM DFPM. During the first round of screening, 62 putative mutants were isolated and they were further tested in a second round of screening. Several criteria were used to select mutants for further studies: i) plants exhibited a wild-type level of ABA-mediated *pRAB18::GFP* reporter expression; ii) plants showed less sensitivity to DFPM inhibition of ABA reporter expression over 3 generations and iii) plants did not show a severe growth defect or morphological alteration throughout developmental stages. Isolated mutant plants were named ***r****esistant to* ***D****FPM-inhibition of* ***A****BA signaling* (*rda*) mutants. Among three *rda* mutants *rda1, rda2* and *rda3* that were isolated during the screen, *rda2* showed the highest reduction in sensitivity to DFPM in leaf epidermal cells (Figure S2).

rda2 is tolerant to DFPM inhibition of ABA signal transduction

rda2 exhibits a reduced sensitivity to DFPM in inhibiting ABA-induced reporter expression (Figure 1). When treated with DFPM and ABA, *rda2* plants showed increased levels of *pRAB18::GFP* fluorescence signal compared to wild-type controls. Confocal microscope images showed enhanced fluorescence in the epidermal layer of true leaves in *rda2* (Figure 1A). The difference between *rda2* and wild-type leaves was clearly visible in epidermal pavement cells where wild-type leaves showed inhibition of ABA-mediated *pRAB18::GFP* fluorescence expression in response to DFPM (Figure 1A, B). In the absence of DFPM, ABA-mediated reporter expression was indistinguishable from *rda2* and wild type leaves. The strong *pRAB18::GFP* fluorescence in guard cells (Figure 1 A, B) has been suggested to result from elevated basal ABA concentration in this cell type (Lahr et al., 1988, Waadt et al., 2014, Waadt et al., 2015, Hsu et al., 2018). The intensity of fluorescence signals was measured from multiple images of leaf epidermal layers showing that *rda2* has a reduced sensitivity to DFPM (Figure 1C).

In addition to the ABA response reporter, other ABA responses of *rda2* were investigated. Treatment of ABA resulted in stomatal closure, whereas pre-exposure to DFPM for 30 min

followed by ABA exposure slightly inhibited ABA-mediated stomatal closing in wild-type leaves at 90 min after ABA treatment (Figure 1D). Time-resolved stomatal movement analyses in intact leaves provide a more robust and kinetic method for investigating stomatal responses (Hsu et al., 2018). Time-resolved stomatal conductance was monitored in intact leaves in the presence of DFPM and ABA by whole leaf gas exchange experiments (Figure 1E). Addition of 2 μM ABA to the transpiration stream via petioles resulted in a rapid decrease in stomatal conductance in wild-type leaves. When wild-type leaves were pre-exposed to DFPM via the transpiration stream for 60 min followed by ABA treatment, stomatal closing in response to ABA was partially inhibited (Figure 1E). Average maximum rates in stomatal conductance reduction in figure 1E were $-0.0385\ min^{-1}$ for wild-type leaves treated with ABA, and $-0.0151\ min^{-1}$ for wild type with DFPM/ABA ($P = 0.002$, two-way ANOVA and Sidak's multiple comparison test). The relatively weaker effect of DFPM in stomatal aperture assays (Figure 1D) is consistent with the effect of DFPM on the kinetics of stomatal closing. In *rda2* mutant leaves, pre-incubation in DFPM did not result in a clear inhibition of ABA-mediated stomatal closing (Figure 1F). Average maximum rates in stomatal conductance reduction were $-0.0232\ min^{-1}$ for *rda2* leaves treated with ABA, and $-0.0306\ min^{-1}$ for *rda2* with DFPM/ABA ($P = 0.279$, two-way ANOVA and Sidak's multiple comparison test), showing reduced sensitivity of *rda2* to DFPM.

ABA-induced gene expression was examined in 2 week-old wild-type and *rda2* plants in the presence or absence of DFPM using real-time quantitative PCR (Figure 1G, H). Pre-exposure of wild-type seedlings to 10 μM DFPM for 1 hour followed by 10 μM ABA exposure for 5 hours or 9 hours inhibited ABA-mediated increase in gene expression (Figure 1G, H). In contrast, *rda2* seedlings exhibited a less severe DFPM inhibition of ABA-induced *RESPONSIVE TO ABA 18* (*RAB18*) and *EARLY RESPONSIVE TO DEHYDRATION10* (*ERD10*) expression at 5 hours after ABA treatment, while there was no clear change at 9 hours after ABA treatment (Figure 1G, H). The described results demonstrate that *rda2* mutants are not impaired in ABA responses, but altered in their ABA responses after DFPM exposure.

rda2 carries a recessive mutation, as F_1 generation plants after backcrossing *rda2* to the parental (*pRAB18::GFP*) wild type plants exhibited wild type-like DFPM sensitivity. When self-pollinating F_1 progeny, 88 F_2 plants among 387 (22.7%, χ^2=1.055) showed *rda2*-like reduced DFPM sensitivity suggesting that *rda2* carries a single recessive mutation. The sequence of the promoter region in the ABA responsive reporter *pRAB18::G*FP was also determined in *rda2* and showed no mutation. This suggests the integrity of the reporter expression construct in *rda2*. *rda2* was not allelic with the other *rda* mutants, *rda1* and *rda3*. Crossing *rda2* with *rda1* resulted in F_1 progeny with a wild-type level DFPM response. As *rda3* was isolated after *rda2* was mapped, the genomic DNA region of the *RDA2* gene was sequenced in *rda3* and no mutation was found.

We investigated whether *rda2* carries any mutation in genes that are necessary for DFPM signaling including core components of diseases resistance signaling, *EDS1* and *PAD4*, co-chaperone genes *SGT1b* and *RAR1*, and the TIR-NB-LRR gene encoding *VICTR* (Kim et al., 2011, Kim et al., 2012). Genomic DNA regions of these 5 genes were PCR-amplified in the *rda2* mutant and sequenced. *rda2* does not carry mutations in *EDS1, PAD4, SGT1b,*

RAR1 and *VICTR1* suggesting that it harbors a mutation in a novel genetic component that is required for the interference signal that inhibits ABA signal transduction by DFPM.

Previous studies showed that *eds1, pad4, sgt1b*, and *rar1* mutants exhibited reduced sensitivity to DFPM in inhibiting ABA-mediated gene expression in whole seedlings (Kim et al., 2011). Note that *victr* mutants have not yet been analyzed for DFPM sensitivity in inhibiting ABA-induced gene expression. *VICTR* expression is strongly induced in roots and *VICTR* is a member of four homologous tandem repeat TIR-NB-LRR genes (Kim et al., 2012). To examine DFPM sensitivity with ABA reporter expression in leaves, mutant plants of *EDS1, PAD4, SGT1b, RAR1, VICTR1* and its closest homolog gene *VICTR Like 1* (*VICTL1*) (Kim et al., 2011, Kim et al., 2012) were introduced with the *pRAB18::GFP* reporter by cross-pollination. The mutant plants showed inhibition of ABA-mediated *pRAB18::GFP* fluorescence levels in epidermal pavement cells in response to DFPM, similarly to the corresponding wild type (Figure S3), showing a difference in whole seedling RT-qPCR analyses of *RAB18* expression (Kim et al., 2011) and leaf pavement cell *pRAB18::GFP* reporter protein activity. These results suggest that *EDS1, PAD4, SGT1b, RAR1, VICTR* and *VICTL1* are not primarily necessary for DFPM inhibition of ABA-mediated *pRAB18::GFP* expression at least in leaf epidermal pavement cells. *rda2* is a single locus exhibiting the strongest DFPM-insensitive mutant phenotype in leaves, whereas VICTR and early ETI signaling components are required for the DFPM response in roots.

Mapping of *rda2* via whole genome sequencing

To map the causative mutation for reduced DFPM sensitivity in *rda2*, the *rda2* mutant plants (named *rda2-1* from here onwards) were backcrossed into the wild-type parent line expressing *pRAB18::GFP*. F_2 plants from self-pollinating F_1 progeny were screened for individuals with an *rda2*-like phenotype showing higher ABA-mediated *pRAB18::GFP* fluorescence levels in leaves pre-treated with DFPM. Eighty-six F_2 plants with reduced sensitivity to DFPM were selected for a mapping population.

Genomic DNA pooled from the 86 F_2 lines of the mapping population was used for whole genome sequencing. The parental Col-0 plants that express the ABA responsive reporter *pRAB18::GFP* and the non-allelic *rda1* mutant were also used for whole genome sequencing for comparison. Single nucleotide polymorphisms (SNPs) of *rda2* also found in the parental line and *rda1* were excluded. Occurrence ratios of *rda2*-specific SNPs and reference type bases for each base position were plotted throughout the five chromosomes of *Arabidopsis thaliana* (Figure 2)(Schneeberger et al., 2009), and showed a clear single peak with high density of *rda2* SNPs in chromosome 1, ranging from 2.2 to 4.8 Mb. This region contains 26 EMS-type C-to-T or G-to-A mutations, and among them 16 mutations resulted amino acid substitutions, premature stop codons or predicted splicing errors (Figure 2, Table S1). None of the 16 genes which carry *rda2*-specific SNPs was reported previously to have a function in ABA signal transduction or immune responses.

T-DNA insertion mutant lines for the 16 genes containing SNPs were used to identify the causative mutation for *rda2*. Homozygous T-DNA knockout lines were tested for DFPM sensitivity in inhibiting ABA-mediated gene expression. We were not able to isolate homozygous mutants in two of the T-DNA lines, *At1g11330* (SALK_143489) and

At1g09750 (GABI_565C02). Instead, their heterozygous lines were crossed with the *rda2* mutant to determine allelism between the causative mutation of *rda2* and the T-DNAs (Figure S4). If any T-DNA is allelic with the *rda2* mutant, F_1 progeny after these crosses would include 50% of plants exhibiting an *rda2*-like DFPM response. When heterozygous plants of the GABI_565C02 T-DNA insertion line, mutated in *At1g09750* were crossed with *rda2*, all F_1 generation plants showed a WT-like DFPM response (Figure S4B). However, half of the F_1 population from the cross between heterozygous SALK_143489 and *rda2* exhibited a phenotype similar to *rda2*, showing a reduced sensitivity to DFPM (Figure S4A). Genotyping of the F_1 lines revealed that half of the F_1 lines showing the *rda2*-like DFPM response carried a T-DNA insertion in *At1g11330*. As a control, the same heterozygous T-DNA insertion line plants (SALK_143489) were crossed with the wild-type parent *pRAB18::GFP* line, and all F_1 plants tested showed wild type-like DFPM sensitivity (Figure S4A). These results suggest that the T-DNA insertion line SALK_143489 in the *At1g11330* gene is allelic to *rda2*. The SALK_143489 line was later named as *rda2-3*.

RDA2 encodes a putative lectin receptor kinase

In *rda2*, a C-to-T mutation in *At1g11330* resulted in change of Glutamine 574 to a premature stop codon (Q574*) (Figure 3A, Table S1). To independently investigate whether *At1g11330* is responsible for the observed phenotypes of the *rda2-1* mutant, an additional homozygous T-DNA insertion line *rda2-2* (SALK_122993) was isolated (Figure 3A). This suggests that the inability to isolate homozygous *rda2-3* (SALK_143489) may result from a linked second site mutation. *rda2-2* was transformed with the ABA response marker *pRAB18::GFP* to examine the DFPM response in inhibiting ABA-mediated reporter expression. Similarly to the *rda2-1* EMS mutant, leaves of the *rda2-2* T-DNA insertion mutant exhibited a wild-type level of ABA-mediated reporter expression (Figure 3B). When treated with DFPM, *rda2-2* showed a reduced sensitivity in inhibiting the ABA-mediated GFP fluorescence signal in epidermal pavement cells of leaves, when compared to wild-type Col-0 plants transformed with the *pRAB18::GFP* reporter (Figure 3B). The ABA-mediated decrease in stomatal conductance was examined in intact wild-type and *rda2-2* leaves after pre-exposure to DFPM or a solvent control (Figure 3C, D). In DFPM-treated wild-type leaves, stomatal closing in response to ABA was partially inhibited compared to the solvent control (Figure 3C). In *rda2-2* leaves, DFPM did not result in a strong inhibition in ABA-induced stomatal closing (Figure 3D). DFPM sensitivity of *rda2-2* was also tested in ABA-mediated gene expression by real-time qPCR. In the wild type, ABA-induced expression of *RAB18* and *ERD10* was inhibited by DFPM (Figure 3E, F). In *rda2-2*, the decrease in ABA-mediated gene expression levels by DFPM was smaller than in the wild type after 1 hour of DFPM pre-treatment followed by 5 hours of ABA treatment (Figure 3E, F). A clear difference was not observed at 9 hours after ABA treatment. Together, these results showed that the *rda2-2* T-DNA insertion line resembles reduced DFPM sensitivity of the *rda2-1* EMS mutant, and suggest that the mutations in the *At1g11330* gene are responsible for the *rda2* phenotypes.

DFPM-mediated immune MAPK activation requires *RDA2*

RDA2 encodes a putative lectin receptor kinase (LecRK) (Figure 3A). Lectin receptor kinases are composed of an extracellular lectin domain known to bind carbohydrates and an

intracellular protein kinase domain, separated by a single hydrophobic transmembrane domain (Figure 3A) (Bellande et al., 2017). In *Arabidopsis thaliana* and other plant species, LecRKs play a role in pathogen-associated molecular pattern (PAMP)-triggered immune signaling (PTI) by perceiving PAMPs or molecules released to the apoplast during pathogen infection (Chrispeels et al., 1991, Chen et al., 2006, Singh et al., 2013, Vaid et al., 2013, Lannoo et al., 2014, Ranf et al., 2015, Bellande et al., 2017, Chen et al., 2017, Wang et al., 2017).

Plants exposed to DFPM activate immune signaling including expression of *Pathogenesis-related 5* (*PR5*) gene in an *EDS1* and *PAD4*-dependent manner (Kim et al., 2011, Kim et al., 2012). Note that *PR5* expression is also induced by PAMPs including flg22 in the PTI response (Asai et al., 2002). Therefore, we analyzed whether DFPM treatment can activate mitogen-activated protein kinases (MAP kinases), which is one of the earliest cellular responses in PTI signaling (Meng et al., 2013, Frei dit Frey et al., 2014). Wild-type plants treated with flagellin 22 (flg22) for 15 min to 2 hours phosphorylated MPK3 and MPK6 at the highest levels at 15 and 30 min after flg22 treatment (Figure 4A). Levels of phosphorylated MPK3 and MPK6 were then reduced (Figure 4A), similarly to previously reported findings for PTI signaling responses (Frei dit Frey et al., 2014). When wild-type Col-0 plants were exposed to DFPM for the same time periods, phosphorylation levels of MAP kinases increased to the highest level at 15 and 30 min after DFPM treatment and then decreased (Figure 4A). The DFPM-mediated activation of MAP kinases was weaker than that mediated by flg22, but the temporal dynamics were comparable (Figure 4A). The lower band of the two phosphorylated MAP kinase bands by DFPM was significantly reduced in the *mpk3-1* mutant allele (Figure 4B) (Wang et al., 2007), whereas the upper band was reduced in the *mpk6-2* mutant (Figure 4B) (Liu et al., 2004) supporting that the two bands are MPK3 and MPK6. These results suggest that DFPM could activate the MAP kinases MPK3 and MPK6 with a time-dependence similar to flg22-triggered MAPK activation.

To determine whether RDA2 functions in DFPM-mediated activation of MAP kinases, *rda2* mutant plants exposed to DFPM were examined along with wild-type plants. Levels of phosphorylated MPK3 and MPK6 were clearly reduced in the *rda2-1* and *rda2-2* mutants treated with DFPM, when compared to wild type (Figures 4C, S5). In some experiments, DFPM activation of MAP kinase phosphorylation remained high in wild type between 15 and 60 minutes (Figure S5). But in these experiments, *rda2* exhibited strong reduction in DFPM-mediated MAP kinase phosphorylation (Figure S5). To examine whether *rda2* mutants are capable of activating MAP kinases upon exposure to other stimuli, *rda2* mutant plants were treated with the pathogen elicitor flg22 (Figure S6A). *rda2* mutant plants showed flg22-mediated phosphorylation in MAP kinases, similar to wild type plants (Figure S6A). These results together show that *rda2* mutants are defective in DFPM-mediated activation of MAP kinases.

To further dissect whether DFPM-mediated activation of MAPKs via RDA2 is affected by genes required for DFPM signaling (Kim et al., 2011, Kim et al., 2012), we investigated mutant plants in *eds1, pad4, eds1 pad4, sgt1b, rar1* and *victr1* (Kim et al., 2012) (Figure 5). The near-isogenic line NIL-Bu-5, which lacks *VICTR, VICTL1* and two tandem homologous *TIR-NB-LRR* genes, was generated by backcrossing *Arabidopsis thaliana*

accession Bu-5 with Col-0 five times (Ariga et al., 2017) and analyzed for DFPM-mediated MAPK activation with the corresponding control (NIL-Col-0) (Ariga et al., 2017). All tested mutants showed phosphorylation of the MAP kinases in response to DFPM, which were comparable to the wild type (Figure 5). Also, the NADPH oxidase genes *RbohD* and *RbohF* that are required for rapid production of ROS upon pathogen infection (Couto et al., 2016) were examined for their involvement in DFPM-mediated MAPK activation. A double mutant allele *rbohD rbohF-F3* (Kwak et al., 2003) did not exhibit a strong reduction in levels of phosphorylated MAP kinases in response to DFPM, when compared to the wild type (Figure 5C). Therefore, *EDS1, PAD4, SGT1B, RAR1, VICTR, RbohD* and *RbohF* appear not to be necessary for DFPM-mediated activation of MAP kinases.

To examine whether DFPM mediates other types of PTI responses, reactive oxygen species (ROS) production in response to DFPM was analyzed, as ROS production is one of the first physiological outputs after PAMP perception (Couto et al., 2016). When leaves of wild type plants were treated with DFPM, levels of ROS production were not clearly distinguishable from ones treated with the solvent control (Figure S6B). Likewise, there was no clear change in ROS production in *rda2* mutant plants treated with DFPM (Figure S6B) suggesting that DFPM does not induce a strong oxidative burst in leaves. We further analyzed the PAMP-induced rapid burst of ROS in *rda2* mutants in response to flg22 or the endogenous Plant Elicitor Peptide 1 (PEP1) (Yamaguchi et al., 2011, Bartels et al., 2015). In *rda2-1* and *rda2-2* mutant plants, ROS production in response to flg22 or PEP1 was not different from that of wild-type plants (Figure S6C). These data provide positive controls for PAMP-induced ROS burst and suggest that RDA2 is not involved in perception of flg22 and PEP1.

To further investigate whether RDA2 is required for DFPM-induced immune-responsive gene expression, transcript levels of PAMP-responsive genes including *PR5, NDR1/HIN-LIKE10* (*NHL10*), cytochrome P450 monooxygenase *CYP81F2* and *FAD-LINKED OXIREDUCTASE* (*FOX*) (Boudsocq et al., 2010, Couto et al., 2016) were examined in wild-type and *rda2-2* mutant plants treated with DFPM (Figure 4D). After 1 to 6 hours of DFPM treatment, the transcript levels of all four genes were induced by DFPM in wild type seedlings. In *rda2-2* seedlings, DFPM-mediated expression of *NHL10, CYP81F2* and *FOX* was severely impaired (Figure 4D). The expression levels of the *PR5* transcript in *rda2-2* were compromised after 3 hours of DFPM treatment, compared to wild type controls (Figure 4D). These results suggest that DFPM induces expression of PAMP-responsive genes, and *RDA2* is important for DFPM-induced expression of PAMP-responsive genes.

In the same time periods, we also investigated whether DFPM induces expression of genes reported to be specifically induced in response to effector-triggered immune (ETI) stimulation (Mine et al., 2018) (Figure 4E). Expression levels of a TIR-NB-LRR gene At1g72940, *WRKY33* and *MPK3* were increased in wild type plants treated with DFPM (Figure 4E). In the *rda2-2* mutant, DFPM-mediated expression of At1g72920 and *WRKY33* was lower than in the wild type at 1 to 4 hours of DFPM treatment. A difference in DFPM-mediated *MPK3* expression between wild type and *rda2-2* plants was observed at 1 and 4 hours after DFPM exposure (Figure 4E). These results suggest that DFPM-mediated induction of the ETI-linked transcript levels At1g72940, *WRKY33* and *MPK3* is partly dependent on *RDA2*.

To assess whether *RDA2* is involved in bacterial resistance, leaves of *rda2-1* and wild type plants were infiltrated with *Pseudomonas syringae* pv. *tomato* strain DC3000 (*Pst*). *Pst* growth at 2 days after infection was not different between *rda2* and the wild type (Figure 6A) suggesting that loss-of-function in *RDA2* alone does not affect *Pst* tolerance in plants. We also tested whether *RDA2* is involved in *Pst* tolerance when leaves are pre-treated with flagellin 22 (flg22). Wild type plants pre-treated with flg22 exhibited increased tolerance to *Pst*. A mutant allele of *FLAGELLIN-SENSITIVE 2* (*FLS2*) that encodes a receptor for flg22 did not show increased tolerance by flg22 pre-treatment (Figure 6B), as described previously (Zipfel et al., 2004). In response to pre-treatment with flg22, *rda2* showed increased tolerance to *Pst* compared to the non-pretreatment control, similarly to the wild type control (Figure 6B), suggesting that RDA2 is not responsible for FLS2-mediated immune signaling. Furthermore, we examined whether DFPM treatment can improve pathogen tolerance *in planta*. Leaves of wild-type and *rda2* plants were infiltrated with DFPM or solvent control at the time as *Pst* treatment (Figure 6C). Wild type plants treated with DFPM did not show a clear change in *Pst* tolerance at 2 and 5 days after infection compared to solvent control (Figure 6C). *rda2* also showed no apparent change in *Pst* growth between DFPM and solvent treatment conditions. The results suggest that DFPM does not enhance plant tolerance to *Pseudomonas syringae* DC 3000 (*Pst*), when infiltrated into leaves. DFPM causes a substantial immune signaling effect in roots (Kim et al., 2012) and future research with diverse root pathogens would be of interest.

Protein kinase activity of RDA2

To investigate whether the putative lectin receptor kinase RDA2 has a protein kinase activity, the intracellular domain that contains the protein kinase domain of RDA2 was fused with an N-terminal StrepII tag and a C-terminal GST tag, and expressed and purified from *Escherichia coli* (Figure 7). *In vitro* kinase analyses revealed that the recombinant intracellular kinase domain of RDA2 exhibits ATP-dependent auto-phosphorylation and trans-phosphorylation activity of the synthetic substrate, myelin basic protein (MyBP) (Figure 7). The protein kinase activity of RDA2 was greatly reduced when the lysine residue K552 in the ATP-binding domain that is conserved within RDA2 and the receptor kinases FLS2 and BRI1-ASSOCIATED RECEPTOR KINASE (BAK1) (Li et al., 2014), was mutated to a glutamic acid (K552E) (Figure 7). The protein kinase activity of the recombinant RDA2 intracellular domain was also reduced by kinase inhibitors K252a (10 μM) and staurosporine (10 μM) (Figure 7). To investigate whether DFPM affects the protein kinase activity of the intracellular kinase domain of RDA2, 50 to 200 μM DFPM was added to protein phosphorylation reactions. DFPM did not increase or decrease the *in vitro* protein kinase activity of the recombinant intracellular kinase domain of RDA2 (Figure 7). This result suggests that the protein kinase activity of the intracellular domain of RDA2 does not directly respond to DFPM.

To analyze involvement of MAP kinase kinase kinase (MAPKKK) and MAP kinase kinase (MAPKK) in DFPM signaling, DFPM-mediated MAPK activation was examined in the presence of inhibitors for MAPKKKs and MAPKKs (Figure 8A). Wild-type plants were treated with DFPM in the presence or absence of GW5074, Sorafenib or PD098059. Sorafenib, an inhibitor for Raf-type MAPKKKs, inhibited DFPM-mediated activation of

MPK3 and MPK6 in wild type plants, while another Raf-type MAPKKK inhibitor GW5074 did not show a clear effect (Figure 8A). The PD098059 MAPKK inhibitor did not abolish DFPM activation of the MAP kinases (Figure 8A). These results suggest that Sorafenib-sensitive Raf-type MAPKKKs may be involved in DFPM-mediated MAP kinase activation.

As DFPM enhanced phosphorylation of MPK3 and MPK6 in an RDA2-dependent manner (Figure 4) and RDA2 is required for DFPM inhibition of ABA signaling (Figures 1, 3), we explored whether MAPK cascades have a role in interfering with ABA signaling by DFPM. A double mutant allele in the MAP kinase kinases *MKK4* and *MKK5* which function upstream of MPK3 and MPK6 (Zhang et al., 2018) was used. When *mkk4-18 mkk5-18* mutant plants (Zhao et al., 2014) were pre-treated with DFPM for 1 hour and treated with ABA for additional 5 hours, ABA-induced transcription of *RAB18* and *ERD10* was less inhibited by DFPM compared to the wild type (Figure 8B). This reduced sensitivity to DFPM suggests roles of *MKK4* and *MKK5* in DFPM-mediated inhibition in ABA signal transduction.

Discussion

The small molecule DFPM activates plant immune signaling and thereby interferes with the ABA signaling pathway (Kim et al., 2011). We aimed to gain further insight into the molecular basis for the DFPM-mediated immune signaling and inhibition in ABA signaling in this study. By screening EMS mutant plants for reduced sensitivity to DFPM in inhibiting ABA-mediated pRAB18::GFP reporter protein expression, we identified *RDA2* that is required for inhibiting ABA signal transduction by DFPM. Two alleles of *rda2* mutant plants exhibited higher levels of ABA-mediated reporter expression in leaves in response to DFPM than the wild type, while responses to ABA were not altered in *rda2* (Figures 1, 3). The *rda2* mutant plants also showed a reduced sensitivity to DFPM in inhibiting ABA responses including ABA-induced stomatal closure and gene expression (Figures 1, 3). Whole genome sequencing based mapping revealed that *RDA2* encodes a previously uncharacterized *Galanthus nivalis* agglutinin-type (G-type) (Bellande et al., 2017) lectin receptor kinase.

DFPM causes signaling in an *EDS1*/*PAD4*/*SGT1b*/*RAR1*-dependent manner (Kim et al., 2011, Kim et al., 2012). Additionally, here we show that DFPM also induces activation of the MAP kinases MPK3 and MPK6 with temporal dynamics similar to flg22-mediated MAPK activation (Figure 4). Activation of MPK3 and MPK6 is one of the earliest signaling responses upon pathogen perception in PAMP-triggered immunity (PTI) (Meng et al., 2013). It is noteworthy that DFPM induces PTI-like responses including MAP kinase activation and gene expression (Figure 4), while DFPM did not induce a rapid ROS burst (Figure S6B). These data suggest that DFPM induces an atypical PTI response. DFPM-mediated MAPK activation was not altered in *eds1, pad4, eds1 pad4, sgt1b, rar1* and *victr* mutants (Figure 5). *EDS1, PAD4, SGT1b, RAR1* and *VICTR* are required for DFPM-mediated ETI signaling, as mutant in these five genes were insensitive to DFPM in inhibiting root growth (Kim et al., 2012, Kunz et al., 2016). Our results suggest that DFPM activation of MAP kinases does not require signaling components of effector-triggered immunity (ETI) mediated immune signaling, and DFPM also mediates components of immune signaling that are not mediated

by EDS1/PAD4-dependent ETI signaling. DFPM activation of ETI mechanisms appears to lie downstream of or parallel to MAPK activation.

Furthermore, we observed that mutant plants of *EDS1, PAD4, SGT1b, RAR1, VICTR* and *VICTL1* showed wild-type levels of DFPM sensitivity in inhibiting ABA-mediated *pRAB18::GFP* reporter protein levels in leaves (Figure S3), which differs from transcript level analyses in whole seedlings (Kim et al., 2011). It is conceivable that the effect of the ETI signaling components is weaker in terms of interference with ABA signaling in leaf pavement cells and ETI signaling may be less central to the DFPM-ABA response. However, a major ETI dependent response of DFPM occurs in roots (Kim et al., 2012, Kunz et al., 2016). Therefore, the present findings in leaves show difference in these responses. DFPM further strongly upregulates the expression of *VICTR* specifically in roots which itself regulates the native *VICTR* gene (Kim et al., 2012, Kunz et al., 2016).

In *rda2* mutants, DFPM-mediated MAPK activation and induction of PAMP-responsive genes were severely abolished (Figure 4C and D). These results suggest that the lectin receptor kinase RDA2 functions in early DFPM signaling thus transducing the signal to downstream pathways including MAPK activation and transcriptional regulation. DFPM-mediated expression of ETI-specific genes was partly dependent on *RDA2* (Figure 4E). Interestingly, *rda2* mutant plants showed a wild-type response to DFPM in inhibiting root growth (Figure S7) suggesting that RDA2 may not be fully involved in DFPM-mediated ETI signaling (Kim et al., 2011, Kim et al., 2012, Kunz et al., 2016). Note however that *RDA2* is a member of 3 tandemly repeated lectin receptor kinase (LecRK) genes and higher order LecRK mutants may need to be investigated in future analyses.

Lectin receptor kinases (LecRKs) activate plant immune signaling by perceiving and sensing molecules in the apoplast that are released from pathogens or released during pathogen infection (Van Holle et al., 2018). There is only a handful of LecRKs whose carbohydrate binding activity has been identified thus far (Willmann et al., 2011, Liu et al., 2012, Kouzai et al., 2014, Ranf et al., 2015). G-type LecRK LIPOOLIGOSACCHARIDE-SPECIFIC REDUCED ELICITATION (LORE) was shown that it can sense lipopolysaccharides (LPS) (Ranf et al., 2015). Recent studies have also shown that LecRK can recognize extracellular ATP and nicotinamide adenine dinucleotide (NAD^+) that could be a sign of pathogen infection (Choi et al., 2014, Wang et al., 2017). This binding activity of LecRKs to non-carbohydrate ligands has been suggested as a result of neofunctionalization of duplicated LecRK genes (Van Holle et al., 2018). Whether RDA2 can perceive the DFPM signal and whether DFPM or its metabolized products can directly bind to RDA2 will require further investigation.

Plasma membrane localization of RDA2 has been suggested by experimental evidence including plasma membrane proteomic studies (Elmore et al., 2012, de Michele et al., 2016, Hooper et al., 2017), and supports a role of RDA2 in perceiving exogenous cues. Our experiments to examine the subcellular localization of the RDA2-GFP fusion protein were not successful due to possible mis-localization at endosomal organelles, because of high expression of the ectopically expressed proteins. A study with a lectin receptor kinase LecRK-I.8 failed to observe LecRK-I.8 fused with GFP in stably transformed plant lines,

suggesting tight regulation of LecRK protein expression (Wang et al., 2017). Furthermore, examining natural ligands of RDA2 will open deeper insights into roles of the LecRK in immune signaling and biotic-to-abscisic acid cross interference signaling.

MAPK cascades transduce and amplify immune signals from receptor kinases (Tena et al., 2011). Here we show that *mkk4 mkk5* double mutant plants exhibited reduced sensitivity to DFPM-mediated inhibition of ABA marker gene expression (Figure 8B). The results suggest that MKK4 and MKK5 are involved in DFPM-mediated inhibition of ABA signal transduction. Further, DFPM-mediated activation of MPK3 and MPK6 was strongly impaired in *rda2* mutant alleles (Figure 4C), which indicates that the lectin receptor kinase RDA2 activates MAPKs MPK3 and MPK6 in response to DFPM. Receptor-like kinases including FLS2 and EF-TU RECEPTOR (EFR) were shown to function upstream of MPK3 and MPK6 (Xu et al., 2015). Rice LecRK SALT INTOLERANCE1 (SIT1) binds and directly phosphorylates rice MAP kinases MPK3 and MPK6 (Li et al., 2014). Rice lysine motif (LysM)-containing receptor kinase OsCERK1 interacts with the receptor-like cytoplasmic kinase RLCK185 which activates rice MPK3 and MPK6 (Kishi-Kaboshi et al., 2010, Yamaguchi et al., 2013). The receptor-like cytoplasmic kinase VII (RLCK VII) together with MAPKKK3 and MAPKKK5 is important for PAMP-induced activation of MPK3 and MPK6 via receptor kinases (Bi et al., 2018). The RDA2 lectin receptor kinase could transduce immune signals to downstream MAPK cascades, and may work with receptor-like cytoplasmic kinases (RLCKs) (Jurca et al., 2008, Bi et al., 2018).

MAPK cascades including MPK3 and MPK6 are thought to be convergence points of PAMP signaling and other immune signaling, since both FLS2- and EFR-mediated PAMP responses and the damage-associated molecular pattern (DAMP) oligogalacturonic acids (OGs) activate MAP kinases (Meng et al., 2013). The exact mechanisms by which MKK4 and MKK5 are involved in biotic-to-abscisic acid interference signaling are yet to be determined. Further investigation using viable loss-of-function mutants of *MPK3* and *MPK6* would help examine their role in this response. Since *rbohd rbohf* double mutant plants did not show an altered response in DFPM-mediated MAPK activation, apoplastic ROS may not function upstream of DFPM-mediated activation of MAP kinases. However, we cannot rule out roles of ROS and NADPH oxidases in cross interference signaling between biotic and abiotic stress signaling transduction in tissues other than those tested in this study. Further characterization of the genes defective in other *rda* mutants will provide additional insights into the molecular mechanisms of DFPM-mediated inhibition of the ABA signal transduction.

In conclusion, the present study identifies the lectin receptor kinase RDA2, which is important for DFPM-mediated immune signaling and interference signaling that inhibits ABA signal transduction. RDA2 is required for transducing the DFPM-mediated signal to activate MAP kinases and subsequently suppress ABA-mediated responses.

Experimental procedures

Plant materials, growth conditions and chemicals

The *Arabidopsis thaliana* accession Columbia-0 (Col-0) was used throughout this study unless indicated otherwise. *Arabidopsis* seeds were surface-sterilized in 70% EtOH and 0.004% SDS for 15 min, then rinsed with 100% EtOH 5 times and sown on 1/2 Murashige and Skoog (MS) media (pH 5.8) supplemented with 1% sucrose and 0.8% Phyto Agar. Plates with sterilized seeds were stratified in the dark for 2 to 3 days at 4 °C and then transferred to a growth chamber under a 16/8 h light/dark cycle at 60-80 μmol/m^2·s^1 light intensity at 19-21 °C.

To generate an ethyl methanesulphonate (EMS)-mutagenized pool, seeds of Col-0 expressing *pRAB18::GFP* were incubated in 1.5 to 3 % EMS overnight and thereafter M2 plants were used for forward genetic screening. *mpk3-1* (SALK_151594), *mpk6-2* (SALK_073907) and *mkk4-18 mpk5-18* were gifts of Prof. Shuqun Zhang (University of Missouri). NIL-Bu-5 and NIL-Col-0 seeds were gifts from Prof. Teruaki Taji (Tokyo University of Agriculture, Japan). *eds1-2, pad4-1, eds1-2 pad4-1, sgt1b* (*eta3*), *rar1-21, victr-1, victl1-1* (Kim et al., 2012) and *rbohd rbohf-f3* (Kwak et al., 2003) were previously reported. To obtain *eds1-2, pad4-1, eds1-2 pad4-1, sgt1b* (*eta3*), *rar1-21, victr-1, victl1-1* mutant plants expressing *pRAB18::GFP*, the mutant plants were crossed with wild-type Col-0 expressing *pRAB18::GFP*. *rda2-2* (SALK_122993), *rda2-3* (SALK_143489), GABI_565C02 and other T-DNA insertion lines were ordered from the Arabidopsis Biological Resource Center. To obtain *rda2-2* expressing *pRAB18::GFP, rda2-2* plants were transformed with *pRAB18::GFP* via *Agrobacterium*-mediated floral dipping. For comparison, wild-type Col-0 plants were also transformed with *pRAB18::GFP* at the same time.

DFPM ([5-(3,4-dichlorophenyl)furan-2-yl]-piperidine-1-ylmethanethione) was purchased from ChemBridge (chemical ID 6015316) and Innovapharm (Ukraine, chemical ID STT-00334837). A 23 amino acid peptide corresponding to AtPep1 active sequence (PEP1) was purchased from Genscript.

ABA response reporter *pRAB18::GFP* microscopy

Arabidopsis plants expressing *pRAB18::GFP* were germinated in ½ MS plates with 1% sucrose and 0.8% Phyto agar, and grown in the growth chamber at 60-80 μmol/m^2·s^1 light intensity at 19-21 °C for 7 days. Plants were then transferred to soil and grown in a growth chamber under a 12/12 h light/dark cycle at 60-80 μmol/m^2·s^1 light intensity at 19-21 °C for additional 7 days. First and second true leaves, the first pair of true leaves developed after cotyledons, were detached and floated on ½ MS liquid medium with 1% sucrose. Each leaf was placed in one well of 96-well plates with its adaxial side up. DFPM was added to a final concentration of 10 μM, and after one hour ABA was added to a final concentration of 20 μM. DMSO was used as a solvent control for DFPM and ethanol (EtOH) was used as a solvent control for ABA. After 24-26 hours of ABA addition, GFP fluorescence signals were observed from abaxial epidermal layers of leaves using confocal microscopes, LSM 800, LSM 710 (Zeiss), or Eclipse TE2000-U (Nikon). Constant gain and pinhole values, or

exposure time were used for each experiment and comparisons of genotypes. Average fluorescence intensity of each image was calculated using Image J software in a genotype and chemical treatment blind manner. Statistical analyses were performed with Prism (Graphpad).

Whole genome sequencing and mapping

Genomic DNA from 86 independent F2 backcrossed lines displaying the *rda2* phenotype was isolated by DNeasy Plant kit (Qiagen). The concentration of gDNA of each F2 line was quantified using Qubit™ dsDNA HS Assay kit and Qubit® Fluorometer (Invitrogen) by the manufacturer's protocol, and equal amounts of gDNA from individual lines were pooled for whole genome sequencing. One μg genomic DNA of the Col-0 *pRAB18::GFP* parental line and of the two *rda* mutants *rda1* and *rda2* was used to construct ~450 bp insert size sequencing libraries with the Truseq Nano DNA kit (Illumina). The three libraries were sequenced in a single lane on an Illumina Hiseq2000 instrument with 2×101-bp paired-ends reads (200-cycle kit v3) and a single 7 bp index read.

Identification of a linked genomic interval and identification of candidate mutations within this interval were done by a custom-made mapping pipeline similar to SHOREmap (Schneeberger et al., 2009). Briefly, paired FASTQ reads were aligned to the *Arabidopsis thaliana* reference genome (TAIR10) by Bowtie 2 (Langmead et al., 2012). Single nucleotide polymorphisms (SNPs) were called by comparison with the reference genome using BCFtools and VCFtools (Danecek et al., 2011). Only EMS type mutations, which are C to T and G to A mutations, were included. SNPs of *rda2* that were also found in the Col-0 *pRAB18::GFP* parental line or *rda1* were excluded. Ratios of *rda2*-specific SNPs over the reference-type base (TAIR 10) were analyzed for every base position by R-values which were quantified by dividing the number of reads with a non-reference base by [the number of reads with a reference base multiplied by the total read number at each position] (Schneeberger et al., 2009). A moving average was calculated to display a candidate interval. Within this interval, mutations were prioritized according to their anticipated effect using the SnpEff tool (Cingolani et al., 2012).

Stomatal movement analyses

Fully expanded leaves of 4-5 week-old plants were detached and floated in stomatal assay buffer (5 mM KCl, 50 μM $CaCl_2$, and 10 mM MES-Tris, pH 5.6) for 2.5 h. Epidermal peels were then prepared using a perforated-tape epidermal detachment method (Ibata et al., 2013). Images of guard cells from the abaxial side of leaves were taken using an inverted light microscope as "Control". The same epidermal peels were then treated with 30 μM DFPM or solvent, and after 30 min ABA was added to a final concentration of 10 μM. 1.5 h after ABA addition, the same guard cells observed in "Control" images were identified and taken as "ABA" or "DFPM/ABA" images. Stomatal apertures were measured using Image J software independently by two different persons in a blind manner. Statistical analyses were performed with Prism (Graphpad).

Whole leaf time-resolved gas exchange analyses

Gas exchange analyses were performed as published previously (Hauser et al., 2018) with mild modification. Briefly, fully expanded rosette leaves of 6-8 week-old plants were cut at the end of the petiole with a fresh razor blade and immediately dipped in water. Another cut was made in the middle of the petiole to avoid clogging of the transpiration stream and petioles were immediately dipped in microcentrifuge tubes with 30 μM DFPM solution. In experiments without DFPM, petioles of detached leaves were dipped in a 0.02% DMSO solution as a solvent control. Stomatal conductance was evaluated using portable gas exchange analyses systems, LI-6800 or LI-6400XT (LI-COR). Detached leaves were clamped with a plant chamber of LI-6800 or LI-6400XT and equilibrated for 40-60 min at a relative humidity of 75%, airflow of 200 rpm and CO_2 concentration of 400 ppm. Once stabilized, steady-state stomatal conductance was measured for 10 min. ABA was then added to a final concentration of 2 μM to the petiole-exposed solution while not touching clamped leaves. Stomatal conductance (mmol $m^{-2}min^{-1}$) was measured for additional 40-60 min. Stomatal conductance is normalized by averages of 10 min steady-state stomatal conductance before ABA addition. Maximum rates of stomatal conductance reduction were analyzed by calculating maximum slopes of each graph and were averaged.

Quantitative gene expression analyses

Two week-old *Arabidopsis* seedlings were treated with 10 μM DFPM for 1 hour, then ABA was added to a final concentration of 10 μM. DMSO was used as a solvent control for DFPM and EtOH was used as a solvent control for ABA. After the indicated time periods, total RNA was extracted using Spectrum™ Plant Total RNA Kit (Sigma-Aldrich), treated with TURBO™ DNase (Thermo-Fisher) and reverse-transcribed using First-Strand cDNA Synthesis Kit (GE Healthcare). qPCR analyses were performed on a BioRad CFX96 qPCR System using SYBR® Green JumpStart (Sigma) with gene specific primers (Table S2). Levels of transcript were normalized against the housekeeping gene *PDF2*. Statistical analyses were performed with Prism (Graphpad).

Measurement of phosphorylated MAP kinases

Ten to fourteen day-old seedlings were incubated in ½ MS liquid media with 1% sucrose containing 30 μM DFPM, 0.06% DMSO (solvent control) or 1 μM flg22 (GenScript) for the indicated time periods. For experiments with kinase inhibitors, plants were pre-treated with 10 μM of GW5074 (Sigma), Sorafenib (Sigma) or PD098059 (Sigma) 30 min before DFPM treatment. Total proteins were extracted in extraction buffer (25 mM Tris-HCl (pH 7.8), 75 mM NaCl, 10 mM $MgCl_2$, 15 mM EGTA, 1 mM DTT, 1 mM NaF, 0.5 mM $NaVO_3$, 15 mM β-glycerolphosphate, 15 mM p-nitrophenylphosphate, 0.1% Tween 20, 0.5 mM phenylmethylsulfonyl fluoride, 5 μg/ml leupeptin). 20 μg of total proteins for each genotype and treatment were subjected to SDS-PAGE. Western blotting was performed with the anti-phospho-p44/42 MAPK (Erk1/2) (Thr202/Tyr204) monoclonal antibody (9101, Cell Signaling Technology) and the secondary anti-rabbit antibody (BioRad) by the manufacturer's protocol. The intensity of phosphorylated MAP kinase bands was quantified using Image J software. The band intensities were presented as ratios to the DFPM control

without inhibitor treatment. Blots were stained with Coomassie blue solution to visualize the amount of loaded proteins.

Recombinant protein purification and *in vitro* kinase assay

The coding sequence of the RDA2 intracellular domain was PCR amplified using RDA2-pGEX-USER-F and RDA2-pGEX-USER-R primers (Table S2), and cloned into the modified pGEX-6P1 vector with a C-terminal GST tag and an additional N-terminal Strep II tag (Brandt et al., 2012) using USER® enzyme (New England Biolabs) resulting in pGEX-6P1-RDA2_intracellular-StrepII. The lysine 552 to glutamic acid mutation (K552E) was introduced to pGEX-6P1-RDA2_intracellular-StrepII by PCR with K552E-F and K552E-R primers (Table S2), resulting in pGEX-6P1-RDA2_intracellular-K552E-StrepII.

Escherichia coli strain BL21 (DE3) was transformed with the plasmids and grown to OD_{600} ~0.6. Protein expression was induced by adding isopropyl-β-D-thiogalactopyranoside (IPTG) to a final concentration of 0.5 mM and growth overnight at room temperature. *E. coli* cells were harvested by centrifugation at 4000 × g for 15 min at 4 °C and resuspended in buffer W (100 mM Tris, 150 mM NaCl, pH 8.0) supplemented with 1 mg/mL lysozyme and protease inhibitor cocktail (Roche). After sonicating *E. coli* cells by three 30-s pulses, insoluble cell debris was removed by centrifugation at 25000 × g for 30 min at 4 °C. RDA2-intracellular domain and RDA2-intracellular-K552E domain proteins were purified with Strep-Tactin® Macroprep® (IBA) following the manufacturer's protocol.

10 ng/μL of recombinant RDA2 intracellular domain was incubated in the phosphorylation buffer (50 mM Tris-HCl pH 7.5, 10 mM $MgCl_2$, 1 mM EGTA, 0.1% Triton X-100, 1 mM DTT) containing 50 ng/μL MyBP together with 50, 100 or 200 μM DFPM or DMSO (control) for 30 min at room temperature. For experiments with kinase inhibitors K252a (Calbiochem) and staurosporine (Sigma), protein samples were pre-incubated with 20 μM of the inhibitors for 30 min before phosphorylation reactions. 200 μM ATP and 0.05 μCi/μL [γ $-^{32}$P]-ATP (PerkinElmer) were then added to start phosphorylation reactions. Phosphorylation reactions were stopped by addition of SDS-PAGE sample buffer after 30 min incubation at room temperature. Phosphorylated proteins were detected by autoradiography after SDS-PAGE.

ROS production measurements

Leaf discs from 3-4 week-old *Arabidopsis* plants were floated on sterile water in white 96-well plates overnight at room temperature under light. At least 12 plants were used per genotype per condition. Each leaf disc was placed in one well of 96-well plates with its adaxial side up. After 20-24 hours, water in 96-well plates was replaced with 50 μL of fresh sterile water and leaf discs were incubated for additional 1 hour. 50 μL of the 2× elicitation solution (100 μg/mL Horseradish Peroxidase (Sigma, P6782), 4 μM L-012 (Wako chemical, 120-04891)) was added to each well. Luminescence was measured with a Mithras LB940 micro plate reader (Berthold). Flg22, PEP1 or DFPM were added to individual wells with a built-in injector in the plate reader to a final concentration of 100 nM flg22, 100 nM PEP1 and 30 μM DFPM. Water control was injected to examine mechanical-induced ROS production. DMSO (0.06%) was used as a solvent control for DFPM.

Pathogen tolerance assays

Pseudomonas syringae pv. tomato DC3000 (*Pst*) culture was grown overnight at 28°C in liquid low salt LB media containing 50 μg/mL rifampicin to the OD_{600} ranging from 0.6 to 1.0. The bacterial cells were collected by centrifugation at 2600 × g for 10 min, room temperature, and resuspended in 10 mM $MgCl_2$ to the OD_{600} of 0.2. The bacterial solution was diluted 1000-fold (10^5 colony forming units per mL) in 10 mM $MgCl_2$ and then infiltrated into the abaxial side of *Arabidopsis* leaves with a needleless syringe. Four week-old Arabidopsis plants were used, and the leaves were either first infiltrated with 1 μM flg22 or H_2O one day prior infiltration with *Pst*, or infiltrated with *Pst* supplemented with 30 μM DFPM or 0.02% v/v DMSO (mock treatment). The inoculated plants were covered with lids to maintain a high humidity. Two 6 mm-diameter leaf disks from eight different plants per treatment were collected and homogenized in 10 mM $MgCl_2$. Serial dilutions were plated on low salt LB agar media containing 50 μg/mL rifampicin and 12.5 μg/mL cycloheximide. The plates were incubated for 2 days at 28°C and the colonies were counted manually.

Supplementary Material

Refer to Web version on PubMed Central for supplementary material.

Acknowledgements

We thank Prof. Shuqun Zhang (University of Missouri) for providing seeds of *mpk3-1* (SALK_151594), *mpk6-2* (SALK_073907) and *mkk4-18 mkk5-18*; Prof. Teruaki Taji (Tokyo University of Agriculture, Japan) for seeds of NIL-Col-0 and NIL-Bu-5. We thank Drs. Detlef Weigel and Christa Lanz (MPI for Developmental Biology, Germany) for sequencing support. We thank Drs. Detlef Weigel (MPI for Developmental Biology, Germany) and Sebastian Schulze (UC San Diego) for critical reading. This research was funded by the National Institutes of Health (GM060396-ES010337) to J.I.S., by Hellman Fellowship to A. H., and partly by the Next-Generation BioGreen 21 Program (SSAC grant PJ01335001), and the Rural Development Administration, Republic of Korea to T.-H. K. J.P. was funded by Human Frontier Science Program Long-term postdoctoral fellowship and K.D. was funded by Ciencias sem Fronteiras/CNPq fellowship (200260/2015-4).

References

Ariga H, Katori T, Tsuchimatsu T, Hirase T, Tajima Y, Parker JE, Alcazar R, Koornneef M, Hoekenga O, Lipka AE, Gore MA, Sakakibara H, Kojima M, Kobayashi Y, Iuchi S, Kobayashi M, Shinozaki K, Sakata Y, Hayashi T, Saijo Y **and** Taji T (2017) NLR locus-mediated trade-off between abiotic and biotic stress adaptation in Arabidopsis. Nat Plants, 3, 17072 10.1038/nplants.2017.72 [PubMed: 28548656] **and**

Asai T, Tena G, Plotnikova J, Willmann MR, Chiu WL, Gomez-Gomez L, Boller T, Ausubel FM **and** Sheen J (2002) MAP kinase signalling cascade in Arabidopsis innate immunity. Nature, 415, 977–83. 10.1038/415977a [PubMed: 11875555] **and**

Asselbergh B, Achuo AE, Hofte M **and** Van Gijsegem F (2008a) Abscisic acid deficiency leads to rapid activation of tomato defence responses upon infection with Erwinia chrysanthemi. Mol Plant Pathol, 9, 11–24. 10.1111/j.1364-3703.2007.00437.x [PubMed: 18705880] **and**

Asselbergh B, De Vleesschauwer D **and** Hofte M (2008b) Global switches and fine-tuning-ABA modulates plant pathogen defense. Mol Plant Microbe Interact, 21, 709–19. 10.1094/MPMI-21-6-0709 [PubMed: 18624635] **and**

Atkinson NJ, Jain R **and** Urwin PE (2015) The Response of Plants to Simultaneous Biotic and Abiotic Stress In Combined Stresses in Plants. (Mahalingam R, ed). Switzerland: Springer International Publishing pp. 181–201.**and**

Atkinson NJ **and** Urwin PE (2012) The interaction of plant biotic and abiotic stresses: from genes to the field. J Exp Bot, 63, 3523–43. 10.1093/jxb/ers100 [PubMed: 22467407]

Audenaert K, De Meyer GB **and** Hofte MM (2002) Abscisic acid determines basal susceptibility of tomato to Botrytis cinerea and suppresses salicylic acid-dependent signaling mechanisms. Plant Physiol, 128, 491–501. 10.1104/pp.010605 [PubMed: 11842153] **and**

Bartels S **and** Boller T (2015) Quo vadis, Pep? Plant elicitor peptides at the crossroads of immunity, stress, and development. J Exp Bot, 66, 5183–93. 10.1093/jxb/erv180 [PubMed: 25911744]

Bellande K, Bono JJ, Savelli B, Jamet E **and** Canut H (2017) Plant Lectins and Lectin Receptor-Like Kinases: How Do They Sense the Outside? Int J Mol Sci, 18 10.3390/ijms18061164**and**

Bhattacharjee S, Halane MK, Kim SH **and** Gassmann W (2011) Pathogen effectors target Arabidopsis EDS1 and alter its interactions with immune regulators. Science, 334, 1405–8. 10.1126/science.1211592 [PubMed: 22158819] **and**

Bi G, Zhou Z, Wang W, Li L, Rao S, Wu Y, Zhang X, Menke FLH, Chen S **and** Zhou JM (2018) Receptor-like Cytoplasmic Kinases Directly Link Diverse Pattern Recognition Receptors to the Activation of Mitogen-activated Protein Kinase Cascades in Arabidopsis. Plant Cell. 10.1105/tpc.17.00981**and**

Bostock RM, Pye MF **and** Roubtsova TV (2014) Predisposition in plant disease: exploiting the nexus in abiotic and biotic stress perception and response. Annu Rev Phytopathol, 52, 517–49. 10.1146/annurev-phyto-081211-172902 [PubMed: 25001451] **and**

Boudsocq M, Willmann MR, Mccormack M, Lee H, Shan L, He P, Bush J, Cheng SH **and** Sheen J (2010) Differential innate immune signalling via Ca2+ sensor protein kinases. Nature, 464, 418–422. [PubMed: 20164835] **and**

Brandt B, Brodsky DE, Xue S, Negi J, Iba K, Kangasjarvi J, Ghassemian M, Stephan AB, Hu H **and** Schroeder JI (2012) Reconstitution of abscisic acid activation of SLAC1 anion channel by CPK6 and OST1 kinases and branched ABI1 PP2C phosphatase action. Proc Natl Acad Sci U S A, 109, 10593–8. 10.1073/pnas.1116590109 [PubMed: 22689970] **and**

Bruce TJA (2010) Tackling the threat to food security caused by crop pests in the new millennium. Food Security, 2, 133–141. 10.1007/s12571-010-0061-8

Buhrow LM, Cram D, Tulpan D, Foroud NA **and** Loewen MC (2016) Exogenous Abscisic Acid and Gibberellic Acid Elicit Opposing Effects on Fusarium graminearum Infection in Wheat. Phytopathology, 106, 986–96. 10.1094/PHYTO-01-16-0033-R [PubMed: 27135677] **and**

Chen D, Cao Y, Li H, Kim D, Ahsan N, Thelen J **and** Stacey G (2017) Extracellular ATP elicits DORN1-mediated RBOHD phosphorylation to regulate stomatal aperture. Nat Commun, 8, 2265 10.1038/s41467-017-02340-3 [PubMed: 29273780] **and**

Chen X, Shang J, Chen D, Lei C, Zou Y, Zhai W, Liu G, Xu J, Ling Z, Cao G, Ma B, Wang Y, Zhao X, Li S **and** Zhu L (2006) A B-lectin receptor kinase gene conferring rice blast resistance. Plant J, 46, 794–804. 10.1111/j.1365-313X.2006.02739.x [PubMed: 16709195] **and**

Choi J, Tanaka K, Cao Y, Qi Y, Qiu J, Liang Y, Lee SY **and** Stacey G (2014) Identification of a plant receptor for extracellular ATP. Science, 343, 290–4. 10.1126/science.343.6168.290 [PubMed: 24436418] **and**

Chrispeels MJ **and** Raikhel NV (1991) Lectins, lectin genes, and their role in plant defense. Plant Cell, 3, 1–9. 10.1105/tpc.3.1.1 [PubMed: 1824332]

Cingolani P, Platts A, Wang Le L, Coon M, Nguyen T, Wang L, Land SJ, Lu X **and** Ruden DM (2012) A program for annotating and predicting the effects of single nucleotide polymorphisms, SnpEff: SNPs in the genome of Drosophila melanogaster strain w1118; iso-2; iso-3. Fly (Austin), 6, 80–92. 10.4161/fly.19695 [PubMed: 22728672] **and**

Couto D **and** Zipfel C (2016) Regulation of pattern recognition receptor signalling in plants. Nat Rev Immunol, 16, 537–52. 10.1038/nri.2016.77 [PubMed: 27477127]

Cutler SR, Rodriguez PL, Finkelstein RR **and** Abrams SR (2010) Abscisic acid: emergence of a core signaling network. Annu Rev Plant Biol, 61, 651–79. 10.1146/annurev-arplant-042809-112122 [PubMed: 20192755] **and**

Danecek P, Auton A, Abecasis G, Albers CA, Banks E, Depristo MA, Handsaker RE, Lunter G, Marth GT, Sherry ST, Mcvean G, Durbin R **and** Genomes Project Analysis, G. (2011) The variant call format and VCFtools. Bioinformatics, 27, 2156–8. 10.1093/bioinformatics/btr330 [PubMed: 21653522] **and**

De Michele R, Mcfarlane HE, Parsons HT, Meents MJ, Lao J, Gonzalez Fernandez-Nino SM, Petzold CJ, Frommer WB, Samuels AL **and** Heazlewood JL (2016) Free-Flow Electrophoresis of Plasma Membrane Vesicles Enriched by Two-Phase Partitioning Enhances the Quality of the Proteome from Arabidopsis Seedlings. J Proteome Res, 15, 900–13. 10.1021/acs.jproteome.5b00876 [PubMed: 26781341] **and**

Deutsch CA, Tewksbury JJ, Tigchelaar M, Battisti DS, Merrill SC, Huey RB **and** Naylor RL (2018) Increase in crop losses to insect pests in a warming climate. Science, 361, 916–919. 10.1126/science.aat3466 [PubMed: 30166490] **and**

Elmore JM, Liu J, Smith B, Phinney B **and** Coaker G (2012) Quantitative proteomics reveals dynamic changes in the plasma membrane during Arabidopsis immune signaling. Mol Cell Proteomics, 11, M111 014555 10.1074/mcp.M111.014555**and**

Fan J, Hill L, Crooks C, Doerner P **and** Lamb C (2009) Abscisic acid has a key role in modulating diverse plant-pathogen interactions. Plant Physiol, 150, 1750–61. 10.1104/pp.109.137943 [PubMed: 19571312] **and**

Finkelstein R (2013) Abscisic Acid synthesis and response. Arabidopsis Book, 11, e0166 10.1199/tab.0166 [PubMed: 24273463]

Fischer R, Byerlee D **and** Edmeades G (2009) Can technology deliver on the yield challenge to 2050? How to feed the World in 2050. Proceedings of a technical meeting of experts, Rome, Italy, 24-26 June 2009, 2009 Food and Agriculture Organization of the United Nations (FAO), pp. 1–48.**and**

Frei Dit Frey N, Garcia AV, Bigeard J, Zaag R, Bueso E, Garmier M, Pateyron S, De Tauzia-Moreau ML, Brunaud V, Balzergue S, Colcombet J, Aubourg S, Martin-Magniette ML **and** Hirt H (2014) Functional analysis of Arabidopsis immune-related MAPKs uncovers a role for MPK3 as negative regulator of inducible defences. Genome Biol, 15, R87 10.1186/gb-2014-15-6-r87 [PubMed: 24980080] **and**

Fujita M, Fujita Y, Noutoshi Y, Takahashi F, Narusaka Y, Yamaguchi-Shinozaki K **and** Shinozaki K (2006) Crosstalk between abiotic and biotic stress responses: a current view from the points of convergence in the stress signaling networks. Curr Opin Plant Biol, 9, 436–42. 10.1016/j.pbi.2006.05.014 [PubMed: 16759898] **and**

Hatfield JL **and** Walthall CL (2015) Meeting Global Food Needs: Realizing the Potential via Genetics x Environment x Management Interactions. Agronomy Journal, 107, 1215–1226. 10.2134/agronj15.0076

Hauser F, Ceciliato PHO, Lin Y-C, Guo D, Gregerson JD, Abbasi N, Youhanna D, Park J, Dubeaux G, Shani E, Poomchongkho N **and** Schroeder JI (2018) A seed resource for screening functionally redundant genes and isolation of new mutants impaired in CO2 and ABA responses. Journal of Experimental Botany. 10.1093/jxb/ery363**and**

Hauser F, Li Z, Waadt R **and** Schroeder JI (2017) SnapShot: Abscisic Acid Signaling. Cell, 171, 1708–1708 e0 10.1016/j.cell.2017.11.045 [PubMed: 29245015] **and**

Hayat Q, Hayat S, Irfan M **and** Ahmad A (2010) Effect of exogenous salicylic acid under changing environment: A review. Environmental and Experimental Botany, 68, 14–25. 10.1016/j.envexpbot.2009.08.005**and**

Heidrich K, Wirthmueller L, Tasset C, Pouzet C, Deslandes L **and** Parker JE (2011) Arabidopsis EDS1 connects pathogen effector recognition to cell compartment-specific immune responses. Science, 334, 1401–4. 10.1126/science.1211641 [PubMed: 22158818] **and**

Hooper CM, Castleden IR, Tanz SK, Aryamanesh N **and** Millar AH (2017) SUBA4: the interactive data analysis centre for Arabidopsis subcellular protein locations. Nucleic Acids Res, 45, D1064–D1074. 10.1093/nar/gkw1041 [PubMed: 27899614] **and**

Hsu PK, Takahashi Y, Munemasa S, Merilo E, Laanemets K, Waadt R, Pater D, Kollist H **and** Schroeder JI (2018) Abscisic acid-independent stomatal CO2 signal transduction pathway and convergence of CO2 and ABA signaling downstream of OST1 kinase. Proc Natl Acad Sci U S A, 115, E9971–E9980. 10.1073/pnas.1809204115 [PubMed: 30282744] **and**

Ibata H, Nagatani A **and** Mochizuki N (2013) Perforated-tape Epidermal Detachment (PED): A simple and rapid method for isolating epidermal peels from specific areas of Arabidopsis leaves. Plant Biotechnology, 30, 497–U112. 10.5511/plantbiotechnology.13.0903b**and**

Jurca ME, Bottka S **and** Feher A (2008) Characterization of a family of Arabidopsis receptor-like cytoplasmic kinases (RLCK class VI). Plant Cell Rep, 27, 739–48. 10.1007/s00299-007-0494-5 [PubMed: 18087702] **and**

Khan MI, Fatma M, Per TS, Anjum NA **and** Khan NA (2015) Salicylic acid-induced abiotic stress tolerance and underlying mechanisms in plants. Front Plant Sci, 6, 462 10.3389/fpls.2015.00462 [PubMed: 26175738] **and**

Kim TH, Hauser F, Ha T, Xue S, Bohmer M, Nishimura N, Munemasa S, Hubbard K, Peine N, Lee BH, Lee S, Robert N, Parker JE **and** Schroeder JI (2011) Chemical genetics reveals negative regulation of abscisic acid signaling by a plant immune response pathway. Curr Biol, 21, 990–7. 10.1016/j.cub.2011.04.045 [PubMed: 21620700] **and**

Kim TH, Kunz HH, Bhattacharjee S, Hauser F, Park J, Engineer C, Liu A, Ha T, Parker JE, Gassmann W **and** Schroeder JI (2012) Natural variation in small molecule-induced TIR-NB-LRR signaling induces root growth arrest via EDS1- and PAD4-complexed R protein VICTR in Arabidopsis. Plant Cell, 24, 5177–92. 10.1105/tpc.112.107235 [PubMed: 23275581] **and**

Kishi-Kaboshi M, Okada K, Kurimoto L, Murakami S, Umezawa T, Shibuya N, Yamane H, Miyao A, Takatsuji H, Takahashi A **and** Hirochika H (2010) A rice fungal MAMP-responsive MAPK cascade regulates metabolic flow to antimicrobial metabolite synthesis. Plant J, 63, 599–612. 10.1111/j.1365-313X.2010.04264.x [PubMed: 20525005] **and**

Kouzai Y, Mochizuki S, Nakajima K, Desaki Y, Hayafune M, Miyazaki H, Yokotani N, Ozawa K, Minami E, Kaku H, Shibuya N **and** Nishizawa Y (2014) Targeted gene disruption of OsCERK1 reveals its indispensable role in chitin perception and involvement in the peptidoglycan response and immunity in rice. Mol Plant Microbe Interact, 27, 975–82. 10.1094/MPMI-03-14-0068-R [PubMed: 24964058] **and**

Kunz HH, Park J, Mevers E, Garcia AV, Highhouse S, Gerwick WH, Parker JE **and** Schroeder JI (2016) Small Molecule DFPM Derivative-Activated Plant Resistance Protein Signaling in Roots Is Unaffected by EDS1 Subcellular Targeting Signal and Chemical Genetic Isolation of victr R-Protein Mutants. PLoS One, 11, e0155937 10.1371/journal.pone.0155937 [PubMed: 27219122] **and**

Kwak JM, Mori IC, Pei ZM, Leonhardt N, Torres MA, Dangl JL, Bloom RE, Bodde S, Jones JD **and** Schroeder JI (2003) NADPH oxidase AtrbohD and AtrbohF genes function in ROS-dependent ABA signaling in Arabidopsis. EMBO J, 22, 2623–33. 10.1093/emboj/cdg277 [PubMed: 12773379] **and**

Lahr W **and** Raschke K (1988) Abscisic-acid contents and concentrations in protoplasts from guard cells and mesophyll cells ofVicia faba L. Planta, 173, 528–531. 10.1007/bf00958966 [PubMed: 24226690]

Langmead B **and** Salzberg SL (2012) Fast gapped-read alignment with Bowtie 2. Nat Methods, 9, 357–9. 10.1038/nmeth.1923 [PubMed: 22388286]

Lannoo N **and** Van Damme EJM (2014) Lectin domains at the frontiers of plant defense. Frontiers in Plant Science, 5 10.3389/fpls.2014.00397

Li CH, Wang G, Zhao JL, Zhang LQ, Ai LF, Han YF, Sun DY, Zhang SW **and** Sun Y (2014) The Receptor-Like Kinase SIT1 Mediates Salt Sensitivity by Activating MAPK3/6 and Regulating Ethylene Homeostasis in Rice. Plant Cell, 26, 2538–2553. 10.1105/tpc.114.125187 [PubMed: 24907341] **and**

Liu B, Li JF, Ao Y, Qu J, Li Z, Su J, Zhang Y, Liu J, Feng D, Qi K, He Y, Wang J **and** Wang HB (2012) Lysin motif-containing proteins LYP4 and LYP6 play dual roles in peptidoglycan and chitin perception in rice innate immunity. Plant Cell, 24, 3406–19. 10.1105/tpc.112.102475 [PubMed: 22872757] **and**

Liu Y **and** Zhang S (2004) Phosphorylation of 1-aminocyclopropane-1-carboxylic acid synthase by MPK6, a stress-responsive mitogen-activated protein kinase, induces ethylene biosynthesis in Arabidopsis. Plant Cell, 16, 3386–99. 10.1105/tpc.104.026609 [PubMed: 15539472]

Mauch-Mani B **and** Mauch F (2005) The role of abscisic acid in plant-pathogen interactions. Curr Opin Plant Biol, 8, 409–14. 10.1016/j.pbi.2005.05.015 [PubMed: 15939661]

Maxmen A (2013) Crop pests: Under attack. Nature, 501, S15–7. 10.1038/501S15a [PubMed: 24067760]

Melillo JM, Richmond TTC **and** Yohe GW (2014) Climate Change Impacts in the United States: The Third National Climate Assessment. U.S. Global Change Research Program, U.S. National Climate Assessment 10.7930/J0Z31WJ2**and**

Meng X **and** Zhang S (2013) MAPK cascades in plant disease resistance signaling. Annu Rev Phytopathol, 51, 245–66. 10.1146/annurev-phyto-082712-102314 [PubMed: 23663002]

Mine A, Seyfferth C, Kracher B, Berens ML, Becker D **and** Tsuda K (2018) The Defense Phytohormone Signaling Network Enables Rapid, High-amplitude Transcriptional Reprogramming During Effector-Triggered Immunity. Plant Cell. 10.1105/tpc.17.00970**and**

Mittler R **and** Blumwald E (2010) Genetic engineering for modern agriculture: challenges and perspectives. Annu Rev Plant Biol, 61, 443–62. 10.1146/annurev-arplant-042809-112116 [PubMed: 20192746]

Mohr PG **and** Cahill DM (2003) Abscisic acid influences the susceptibility of Arabidopsis thaliana to Pseudomonas syringae pv. tomato and Peronospora parasitica. Functional Plant Biology, 30, 461–469. 10.1071/Fp02231

Mosher S, Moeder W, Nishimura N, Jikumaru Y, Joo SH, Urquhart W, Klessig DF, Kim SK, Nambara E **and** Yoshioka K (2010) The lesion-mimic mutant cpr22 shows alterations in abscisic acid signaling and abscisic acid insensitivity in a salicylic acid-dependent manner. Plant Physiol, 152, 1901–13. 10.1104/pp.109.152603 [PubMed: 20164209] **and**

Németh M, Janda T, Horváth E, Páldi E **and** Szalai G (2002) Exogenous salicylic acid increases polyamine content but may decrease drought tolerance in maize. Plant Science, 162, 569–574. 10.1016/s0168-9452(01)00593-3**and**

Oerke EC (2005) Crop losses to pests. The Journal of Agricultural Science, 144, 31 10.1017/s0021859605005708

Olson AJ, Pataky JK, Darcy CJ **and** Ford RE (1990) Effects of Drought Stress and Infection by Maize-Dwarf Mosaic-Virus on Sweet Corn. Plant Disease, 74, 147–151. 10.1094/Pd-74-0147**and**

Park SY, Fung P, Nishimura N, Jensen DR, Fujii H, Zhao Y, Lumba S, Santiago J, Rodrigues A, Chow TF, Alfred SE, Bonetta D, Finkelstein R, Provart NJ, Desveaux D, Rodriguez PL, Mccourt P, Zhu JK, Schroeder JI, Volkman BF **and** Cutler SR (2009) Abscisic acid inhibits type 2C protein phosphatases via the PYR/PYL family of START proteins. Science, 324, 1068–71. 10.1126/science.1173041 [PubMed: 19407142] **and**

Prasch CM **and** Sonnewald U (2013) Simultaneous application of heat, drought, and virus to Arabidopsis plants reveals significant shifts in signaling networks. Plant Physiol, 162, 1849–66. 10.1104/pp.113.221044 [PubMed: 23753177]

Ramegowda V **and** Senthil-Kumar M (2015) The interactive effects of simultaneous biotic and abiotic stresses on plants: mechanistic understanding from drought and pathogen combination. J Plant Physiol, 176, 47–54. 10.1016/j.jplph.2014.11.008 [PubMed: 25546584]

Ranf S, Gisch N, Schaffer M, Illig T, Westphal L, Knirel YA, Sanchez-Carballo PM, Zahringer U, Huckelhoven R, Lee J **and** Scheel D (2015) A lectin S-domain receptor kinase mediates lipopolysaccharide sensing in Arabidopsis thaliana. Nat Immunol, 16, 426–33. 10.1038/ni.3124 [PubMed: 25729922] **and**

Schneeberger K, Ossowski S, Lanz C, Juul T, Petersen AH, Nielsen KL, Jorgensen JE, Weigel D **and** Andersen SU (2009) SHOREmap: simultaneous mapping and mutation identification by deep sequencing. Nat Methods, 6, 550–1. 10.1038/nmeth0809-550 [PubMed: 19644454] **and**

Singh P **and** Zimmerli L (2013) Lectin receptor kinases in plant innate immunity. Front Plant Sci, 4, 124 10.3389/fpls.2013.00124 [PubMed: 23675375]

Suzuki N, Rivero RM, Shulaev V, Blumwald E **and** Mittler R (2014) Abiotic and biotic stress combinations. New Phytol, 203, 32–43. 10.1111/nph.12797 [PubMed: 24720847] **and**

Tena G, Boudsocq M **and** Sheen J (2011) Protein kinase signaling networks in plant innate immunity. Curr Opin Plant Biol, 14, 519–29. 10.1016/j.pbi.2011.05.006 [PubMed: 21704551] **and**

Ton J, Flors V **and** Mauch-Mani B (2009) The multifaceted role of ABA in disease resistance. Trends Plant Sci, 14, 310–7. 10.1016/j.tplants.2009.03.006 [PubMed: 19443266] **and**

Toth R **and** Van Der Hoorn RA (2010) Emerging principles in plant chemical genetics. Trends Plant Sci, 15, 81–8. 10.1016/j.tplants.2009.11.005 [PubMed: 20036182]

Ulferts S, Delventhal R, Splivallo R, Karlovsky P **and** Schaffrath U (2015) Abscisic acid negatively interferes with basal defence of barley against Magnaporthe oryzae. BMC Plant Biol, 15, 7 10.1186/s12870-014-0409-x [PubMed: 25604965] **and**

Vaid N, Macovei A **and** Tuteja N (2013) Knights in action: lectin receptor-like kinases in plant development and stress responses. Mol Plant, 6, 1405–18. 10.1093/mp/sst033 [PubMed: 23430046] **and**

Van Holle S **and** Van Damme EJM (2018) Signaling through plant lectins: modulation of plant immunity and beyond. Biochem Soc Trans, 46, 217–233. 10.1042/BST20170371 [PubMed: 29472368]

Waadt R, Hitomi K, Nishimura N, Hitomi C, Adams SR, Getzoff ED **and** Schroeder JI (2014) FRET-based reporters for the direct visualization of abscisic acid concentration changes and distribution in Arabidopsis. Elife, 3, e01739 10.7554/eLife.01739 [PubMed: 24737861] **and**

Waadt R, Hsu PK **and** Schroeder JI (2015) Abscisic acid and other plant hormones: Methods to visualize distribution and signaling. BioEssays, 37, 1338–1349. 10.1002/bies.201500115 [PubMed: 26577078] **and**

Wang C, Zhou M, Zhang X, Yao J, Zhang Y **and** Mou Z (2017) A lectin receptor kinase as a potential sensor for extracellular nicotinamide adenine dinucleotide in Arabidopsis thaliana. Elife, 6 10.7554/eLife.25474**and**

Wang H, Ngwenyama N, Liu Y, Walker JC **and** Zhang S (2007) Stomatal development and patterning are regulated by environmentally responsive mitogen-activated protein kinases in Arabidopsis. Plant Cell, 19, 63–73. 10.1105/tpc.106.048298 [PubMed: 17259259] **and**

Wang W, Vinocur B **and** Altman A (2003) Plant responses to drought, salinity and extreme temperatures: towards genetic engineering for stress tolerance. Planta, 218, 1–14. 10.1007/s00425-003-1105-5 [PubMed: 14513379] **and**

Willmann R, Lajunen HM, Erbs G, Newman MA, Kolb D, Tsuda K, Katagiri F, Fliegmann J, Bono JJ, Cullimore JV, Jehle AK, Gotz F, Kulik A, Molinaro A, Lipka V, Gust AA **and** Nurnberger T (2011) Arabidopsis lysin-motif proteins LYM1 LYM3 CERK1 mediate bacterial peptidoglycan sensing and immunity to bacterial infection. Proc Natl Acad Sci U S A, 108, 19824–9. 10.1073/pnas.1112862108 [PubMed: 22106285] **and**

Xu J **and** Zhang S (2015) Mitogen-activated protein kinase cascades in signaling plant growth and development. Trends Plant Sci, 20, 56–64. 10.1016/j.tplants.2014.10.001 [PubMed: 25457109]

Yamaguchi K, Yamada K, Ishikawa K, Yoshimura S, Hayashi N, Uchihashi K, Ishihama N, Kishi-Kaboshi M, Takahashi A, Tsuge S, Ochiai H, Tada Y, Shimamoto K, Yoshioka H **and** Kawasaki T (2013) A receptor-like cytoplasmic kinase targeted by a plant pathogen effector is directly phosphorylated by the chitin receptor and mediates rice immunity. Cell Host Microbe, 13, 347–57. 10.1016/j.chom.2013.02.007 [PubMed: 23498959] **and**

Yamaguchi Y **and** Huffaker A (2011) Endogenous peptide elicitors in higher plants. Curr Opin Plant Biol, 14, 351–7. 10.1016/j.pbi.2011.05.001 [PubMed: 21636314]

Yasuda M, Ishikawa A, Jikumaru Y, Seki M, Umezawa T, Asami T, Maruyama-Nakashita A, Kudo T, Shinozaki K, Yoshida S **and** Nakashita H (2008) Antagonistic interaction between systemic acquired resistance and the abscisic acid-mediated abiotic stress response in Arabidopsis. Plant Cell, 20, 1678–1692. 10.1105/tpc.107.054296 [PubMed: 18586869] **and**

Zhang M, Su J, Zhang Y, Xu J **and** Zhang S (2018) Conveying endogenous and exogenous signals: MAPK cascades in plant growth and defense. Curr Opin Plant Biol, 45, 1–10. 10.1016/j.pbi.2018.04.012 [PubMed: 29753266] **and**

Zhao C, Nie H, Shen Q, Zhang S, Lukowitz W **and** Tang D (2014) EDR1 physically interacts with MKK4/MKK5 and negatively regulates a MAP kinase cascade to modulate plant innate immunity. PLoS Genet, 10, e1004389 10.1371/journal.pgen.1004389 [PubMed: 24830651] **and**

Zipfel C, Robatzek S, Navarro L, Oakeley EJ, Jones JD, Felix G **and** Boller T (2004) Bacterial disease resistance in Arabidopsis through flagellin perception. Nature, 428, 764 10.1038/nature02485 [PubMed: 15085136] **and**

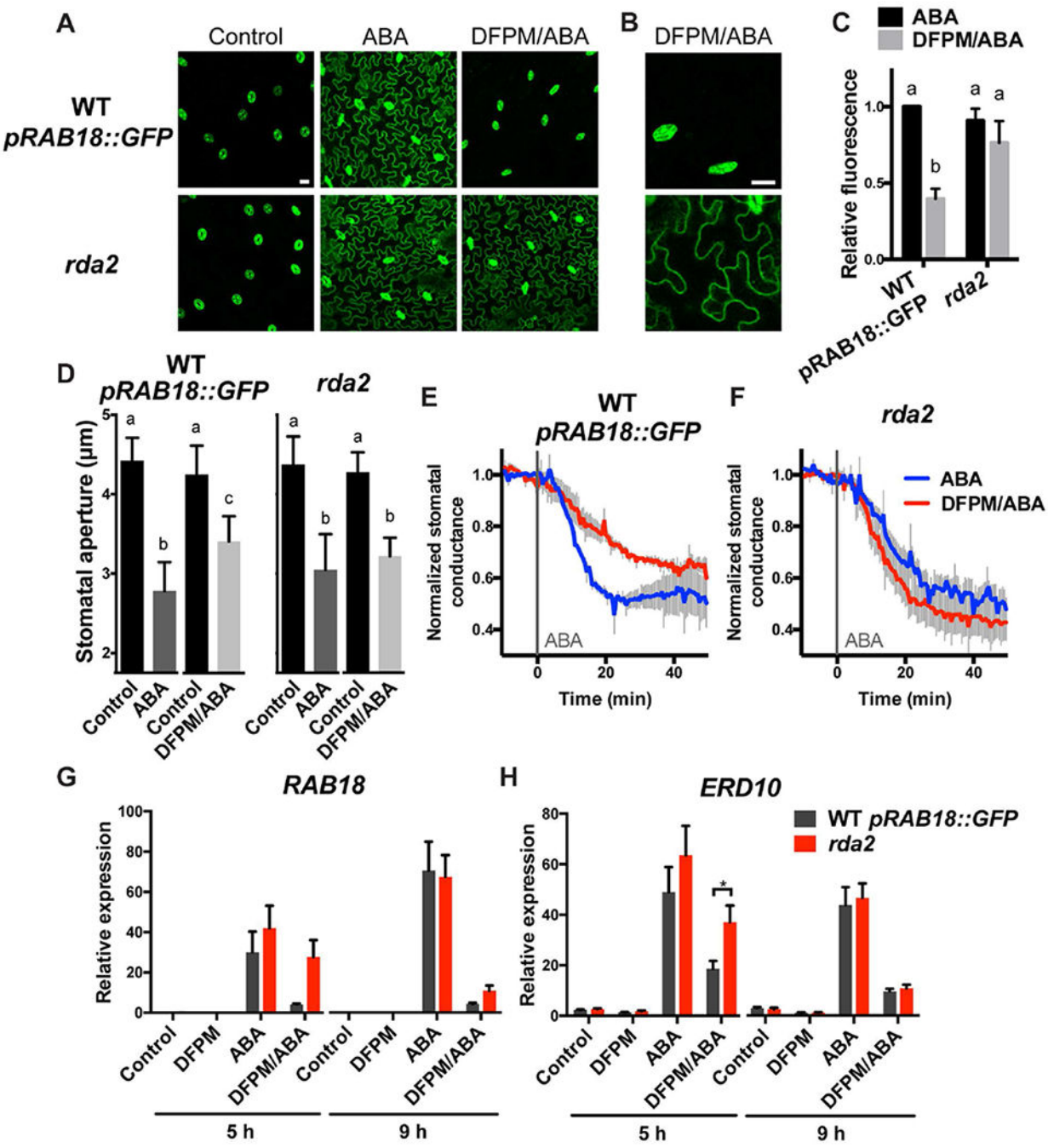

Figure 1. *rda2* exhibits reduced sensitivity to DFPM.

(A) ABA-mediated *pRAB18::GFP* fluorescence levels were less inhibited by DFPM in epidermal pavement cells of *rda2* leaves, when compared to those of wild-type Col-0 expressing *pRAB18::GFP* (WT *pRAB18::GFP*). First and second true leaves of two week-old plants were pre-treated with 10 μM DFPM or solvent control for 1 hour, and then 20 μM ABA or solvent control was added. GFP fluorescence was observed from abaxial epidermal layers of leaves using a confocal microscope after 24-26 hours of ABA addition. Scale bar, 20 μm. Representative images from at least 5 biological repeats are shown. **(B)** Enlarged

images of leaf epidermal layers treated with ABA and DFPM. Scale bar, 20 μm. **(C)** The intensity of *pRAB18::GFP* fluorescence signal in *rda2* and wild type treated with ABA and/or DFPM was quantified. Averages of 5-8 independent experiments, and each are averages of 5-27 images of 3-9 plants per condition per genotype. Data were normalized to the fluorescence intensity of the wild type treated with ABA for each experiment. Error bars = SEM. Asterisk represents $P < 0.05$ based on two-way ANOVA and Sidak's test. **(D)** Effect of DFPM in ABA-induced stomatal closing. Stomatal apertures were measured before (Control) and after 30 min treatment of solvent control or 30 μM DFPM followed with additional 1.5 h treatment of 10 μM ABA (ABA or DFPM/ABA, respectively). Each control bar and their corresponding right bar represent the average widths of the same apertures before and after the chemical treatment, respectively. n = 4 independent experiments, each experiments: 10-27 stomates. Error bars = SEM. Means with different letters are grouped based on two-way ANOVA and Sidak's test, $P < 0.05$. **(E-F)** Time resolved stomatal conductance of wild type **(E)** and *rda2* **(F)** in response to DFPM and ABA. Leaves were pre-treated with 30 μM DFPM or DMSO solvent control via the transpiration stream, and after 60 min 2 μM ABA was added at time=0 (grey line). Stomatal conductance was measured for an additional 50 min. Data are averages of three independent biological repeats, and error bars are SEM. Stomatal conductance was normalized by averaging 10 min steady-state stomatal conductance before ABA addition. **(G-H)** ABA-mediated gene expression was less inhibited by DFPM in *rda2*. Expression levels of ABA responsive *RAB18* **(G)** and *ERD10* **(H)** in wild-type and *rda2* plants were monitored via real-time qPCR after pre-treated with 30 μM DFPM or solvent control for 1 hour and then incubated in 10 μM ABA or solvent control for the indicated time points. Expression levels were normalized with the housekeeping gene *PDF2*. Results are averages of n=4 biological replicates. Asterisk represents $P < 0.05$ based on two-way ANOVA and Sidak's test.

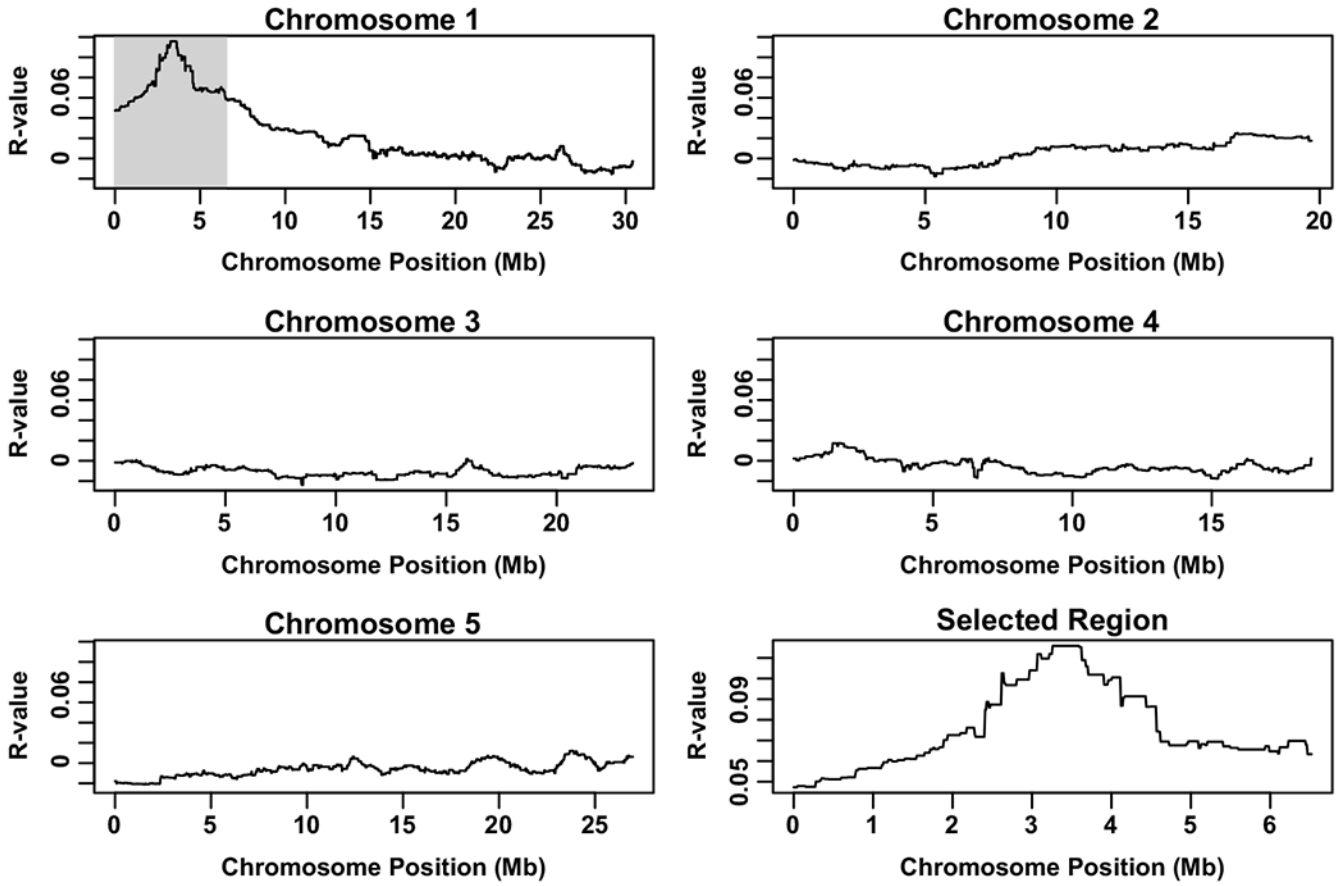

Figure 2. Genome-wide SNPs of *rda2* identified by whole genome sequencing-based mapping.

rda2-specific single nucleotide polymorphisms (SNPs) were identified from whole genome sequencing of *rda2* mapping population and the corresponding wild type Col-0 expressing *pRAB18::GFP*. Occurrence ratios of *rda2*-specific SNPs and wild-type reference bases (TAIR 10) for each base position were plotted through the five *Arabidopsis thaliana* chromosomes. Note that the gray area of chromosome 1 shows a peak with higher ratios of *rda2*-specific SNPs. This area is shown in the right bottom graph in detail. Y axis: R-values of each base position. R-values are calculated by dividing the number of reads with a non-reference base by [the number of reads with a reference base multiplied by the total read number at each position] as previously reported (Schneeberger et al., 2009).

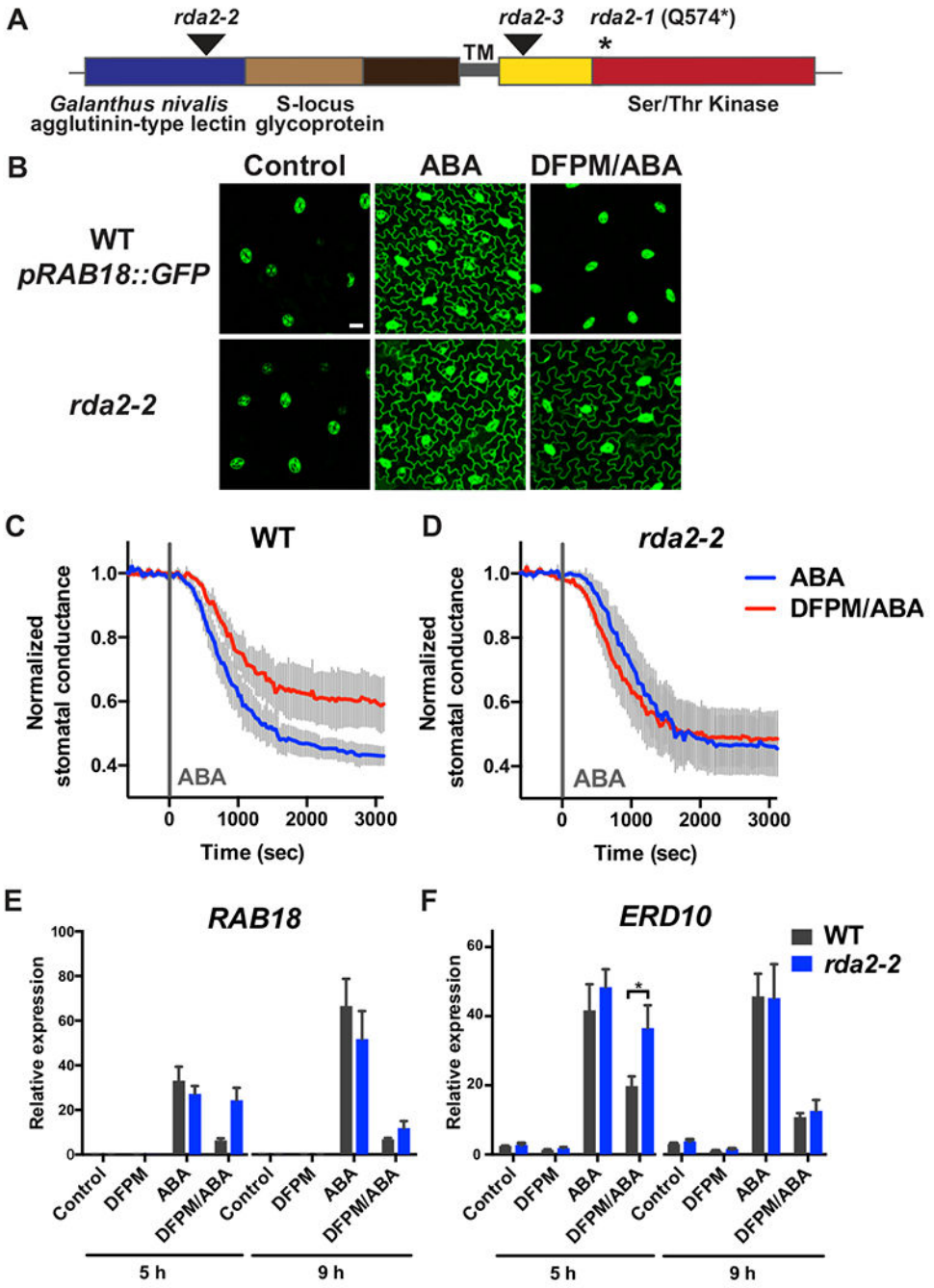

Figure 3. Identification of *RDA2* as a putative lectin receptor kinase gene.

(A) Location of the causative mutation in *rda2-1* (*) and T-DNA insertion (arrowheads) in *rda2-2* and *rda2-3* mutant alleles. Predicted protein domains including a lectin domain and a protein kinase domain in RDA2 are also presented. **(B)** DFPM-mediated inhibition of ABA reporter *pRAB18::GFP* expression was less pronounced in leaf epidermal pavement cells of *rda2-2* compared to the wild type Col-0 expressing *pRAB18::GFP* (WT *pRAB18::GFP*). First and second true leaves of 2 week-old plants expressing *pRAB18::GFP* were pre-treated with DFPM or solvent control for 1 hour and then 20 μM ABA or solvent control was added.

After 24-26 hours of ABA addition, GFP fluorescence signals were observed from abaxial epidermal layers of leaves using a confocal microscope. Scale bar, 20 μm. Representative images from at least 3 biological repeats are shown. **(C-D)** *rda2-2* exhibited reduced sensitivity to DFPM-mediated inhibition of ABA-induced stomatal closing. Leaves of Col-0 wild type **(C)** and *rda2-2* **(D)** were pre-treated with 30 μM DFPM or solvent control for 60 min, and then treated with 2 μM ABA treatment at time=0 (grey line) via the transpiration stream. Stomatal conductance was measured for an additional 50 min. Data are averages of 3-4 independent biological replicates, and error bars are SEM. Stomatal conductance is normalized by averages of 10 min steady-state stomatal conductance before ABA addition. **(E-F)** ABA-induced expression levels of *RAB18* **(E)** and *ERD10* **(F)** were less suppressed by DFPM in *rda2-2* mutants than in wild type plants. For real-time qPCR, plants were pre-treated with 30 μM DFPM or solvent control for 1 h and then incubated in 10 μM ABA or solvent control for the indicated time points. Expression levels were normalized with the housekeeping gene *PDF2*. Results are averages of n=4 biological repeats. Error bars = SEM. Asterisk represents $P < 0.05$ based on two-way ANOVA and Sidak's test.

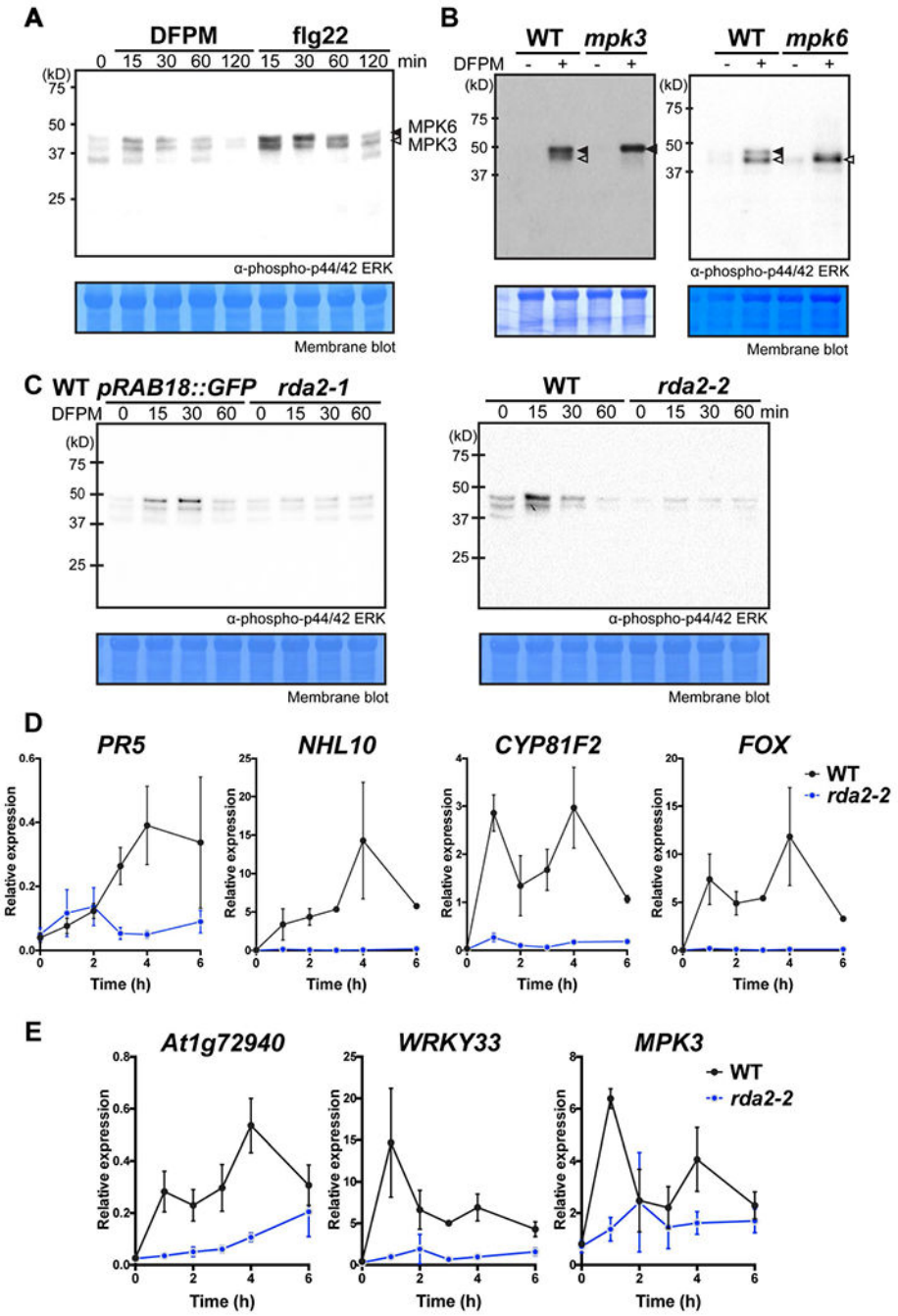

Figure 4. Involvement of *RDA2* in DFPM-mediated PAMP-triggered immune signaling.

(A) DFPM activates MAP kinases (MPKs) within 15 min in wild-type plants. Arrowheads represent two MAP kinases, MPK3 and MPK6, which were activated by flg22. Wild-type Col-0 plants were treated with 30 μM DFPM or 1 μM flagellin 22 (flg22) for the indicated time periods. Whole proteins were used for Western blotting with anti-phospho-p44/42 MAPK (Erk1/2) (Thr202/Tyr204) antibody (α-phospho-p44/42 ERK). Loading controls: coomassie blue staining of the membrane. A representative blot from three biological repeats is shown. **(B)** The lower band of the two bands (open arrowheads) shown in DFPM-

treated wild type plants was reduced in the *mpk3-1* mutant. The upper band (filled arrowheads) was weaker in the *mpk6-2* mutant. Plants were treated with 30 μM DFPM or solvent control for 30 min. **(C)** DFPM-mediated activation of MAP kinases was diminished in *rda2-1* and *rda2-2* mutants compared to the corresponding wild-type plants. Col-0 expressing *pRAB18::GFP* (WT *pRAB18::GFP*) was used as a wild-type control for *rda2-1* and Col-0 (WT) was used as a wild-type control for *rda2-2*. Plants were treated with 30 μM DFPM for the indicated time periods. **(D)** Transcription of PAMP-responsive genes *PR5, NHL10, CYP81F2* and *FOX* was induced by DFPM in wild type plants. DFPM-induced gene expression was strongly impaired in the *rda2-2* mutant. For real-time qPCR, plants were treated with 30 μM DFPM for 1, 2, 3, 4 and 6 hours. Expression levels were normalized with the housekeeping gene *PDF2*. n=3 biological replicates. Error bars = SEM. **(E)** Expression of ETI-specific genes (Mine et al., 2018) a TIR-NB-LRR gene At1g72940, *WRKY33* and *MPK3* was induced by DFPM in the wild type. DFPM-mediated induction of these genes is partly impaired in *rda2-2*. Real-time qPCR was performed as in **(D)**. n=3 biological replicates. Error bars = SEM.

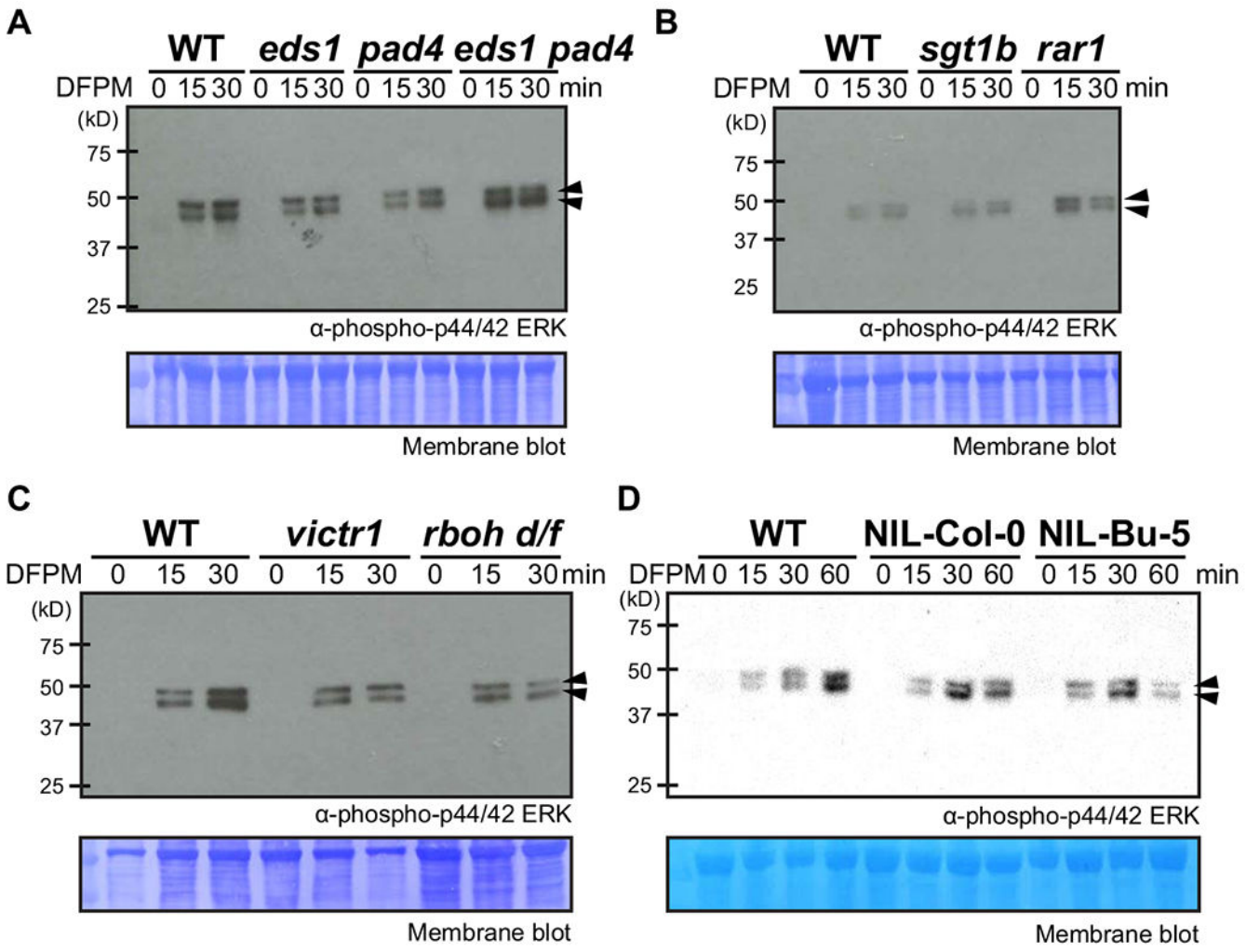

Figure 5. DFPM-mediated activation of MAP kinases in immune-deficient and DFPM signaling-deficient mutants.

DFPM-mediated activation of MAP kinases was examined in *eds1, pad4, eds1 pad4* **(A)**, *sgt1b, rar1* **(B)**, *victr1*, and *rbohd rbohf* **(C)** mutants. A near-isogenic line of Col-0 and Bu-5 that lacks *VICTR* and 3 homolog TIR-NB-LRR genes (NIL-Bu-5) and its corresponding control (NIL-Col-0) **(D)** plants were also tested. Col-0 was used as wild type (WT). None of the tested mutants exhibited a clear alteration in DFPM-mediated activation of MAP kinases (arrowheads). Plants were treated with 30 μM DFPM for the indicated time points and used for whole protein extraction and subsequent Western blotting. Phosphorylated MAP kinases were detected using anti-phospho-p44/42 MAPK (Erk1/2) (Thr202/Tyr204) antibody. Loading controls: coomassie blue staining of membranes. Representative results from three independent repeats are shown.

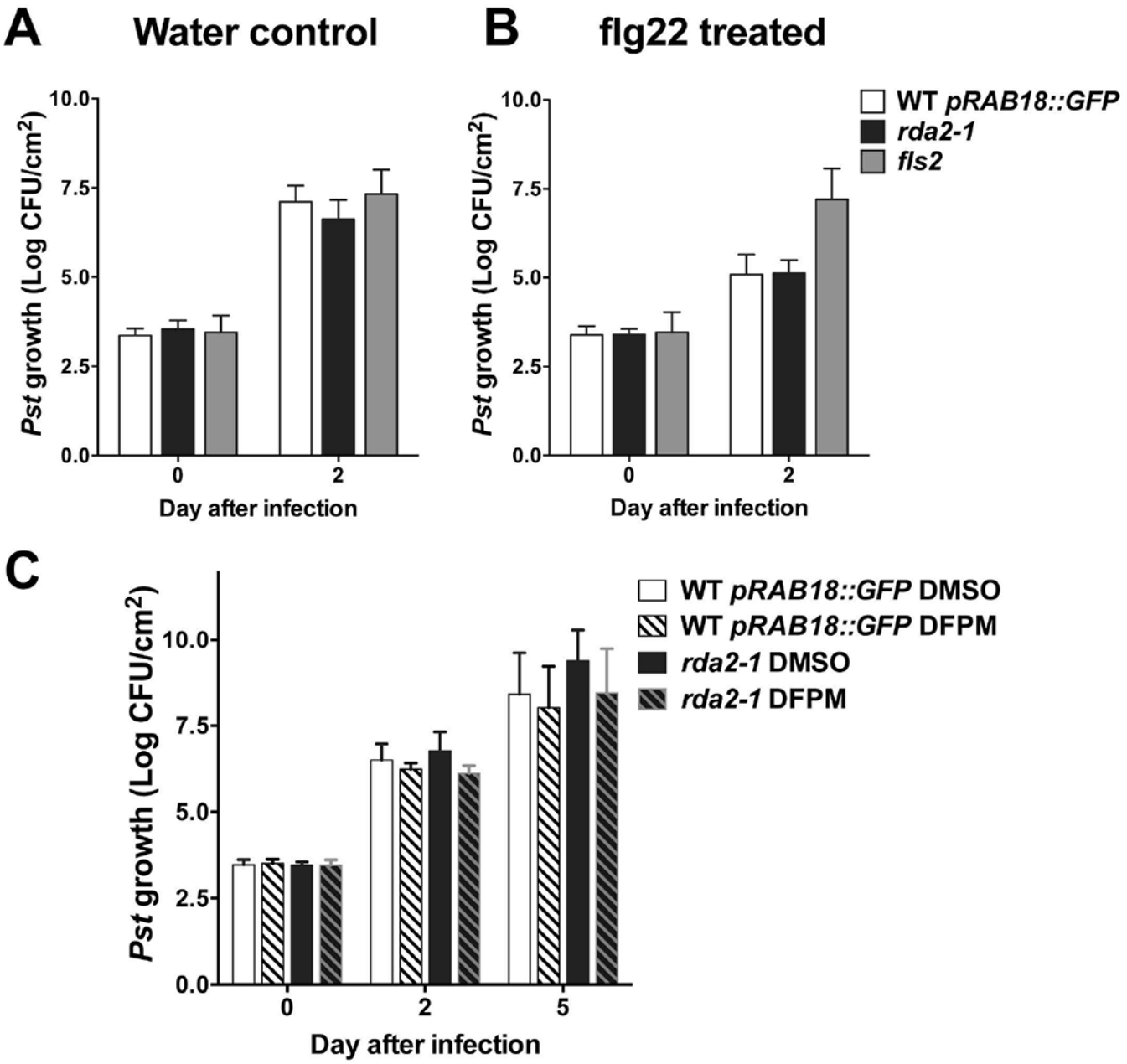

Figure 6. Growth of syringe-infiltrated *Pseudomonas syringae* pv. *tomato* DC3000 (*Pst*) in rosette leaves.

(A-B) Leaves of *rda2-1*, wild-type and *fls2* plants were infiltrated with 1 μM flg22 **(B)** or water control **(A)**, and after one day the same leaves were infiltrated with *Pst*. Growth of bacteria was determined at the indicated time points. n=4 independent experiments for WT and *rda2-1* and n=3 for *fls2*. Each experiment contains 7-8 plants per genotype. Error bars = SEM. **(C)** Leaves of *rda2-1* and wild-type plants were infiltrated with 30 μM DFPM or solvent control when treated with *Pst*. Growth of bacteria was determined at the indicated time points. Two-way ANOVA and Tukey's test showed no difference between genotypes.

n=3 independent experiments which contain 8 plants per genotype. Error bars = SEM. CFU: colony-forming units.

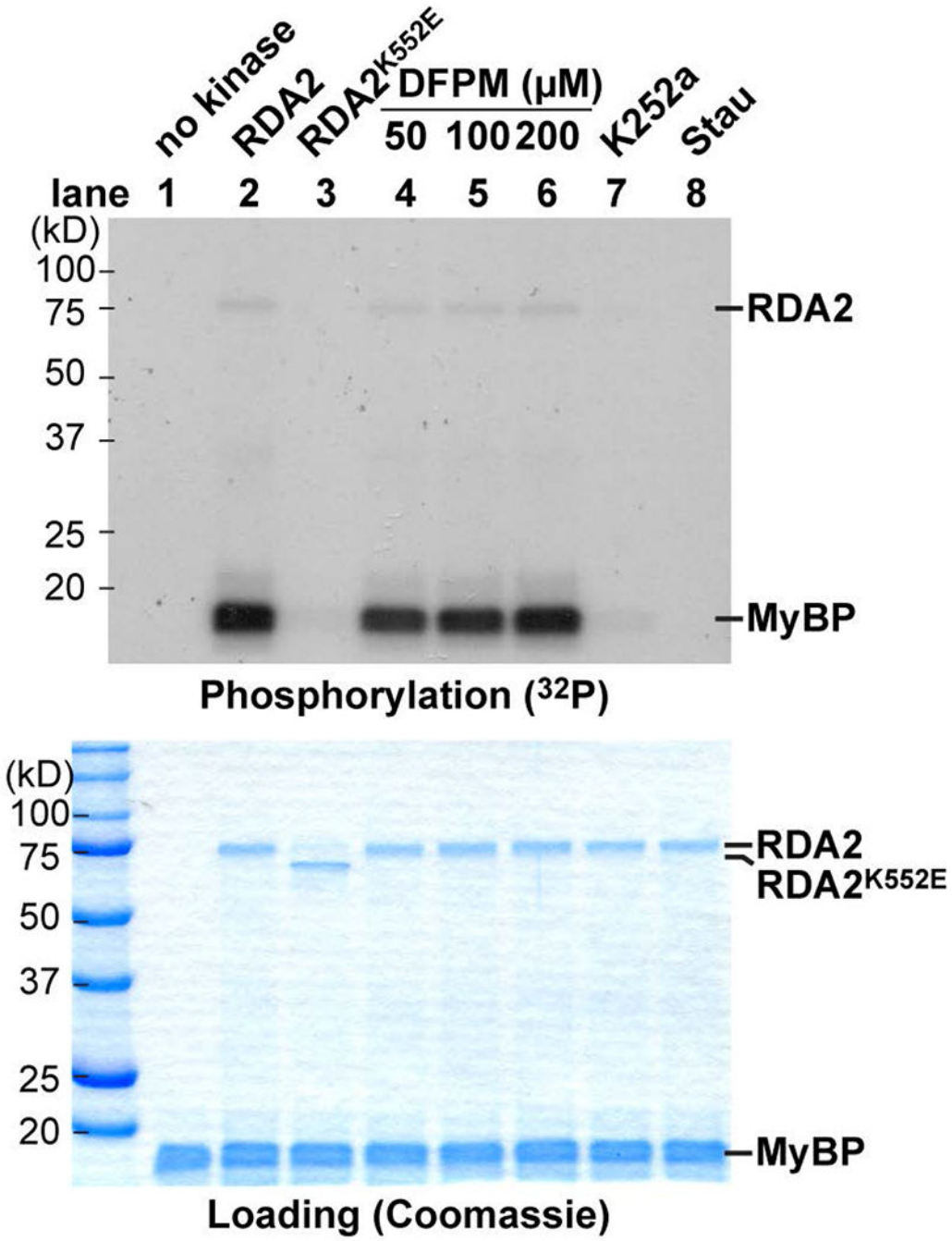

Figure 7. Protein kinase activity of RDA2.

(Lane 1-2) The recombinant intracellular kinase domain of RDA2 exhibited an autophosphorylation activity and a trans-phosphorylation activity to a synthetic substrate myelin basic proteins (MyBP). The intracellular kinase domain of RDA2 was expressed in *E. coli*, purified and used for *in vitro* phosphorylation assay with [γ-^{32}P]-ATP. Phosphorylated proteins were detected by autoradiography after SDS-PAGE. **(Lane 3)** The kinase activity of the recombinant RDA2 protein was strongly diminished, when a conserved lysine residue in the ATP binding domain was mutated to a glutamic acid (K552E). Note

that K552E mutation resulted in a slight shift of the recombinant protein on SDS-PAGE gel. **(Lanes 4-6)** Addition of 50 to 200 μM DFPM to phosphorylation assay reactions did not alter the kinase activity of the recombinant intracellular kinase domain of RDA2. **(Lanes 7-8)** Pre-incubation with protein kinases K252a and staurosporine (Stau) for 30 min before phosphorylation reactions suppressed the kinase activity of RDA2. Loading control: coomassie blue staining of SDS-PAGE gel.

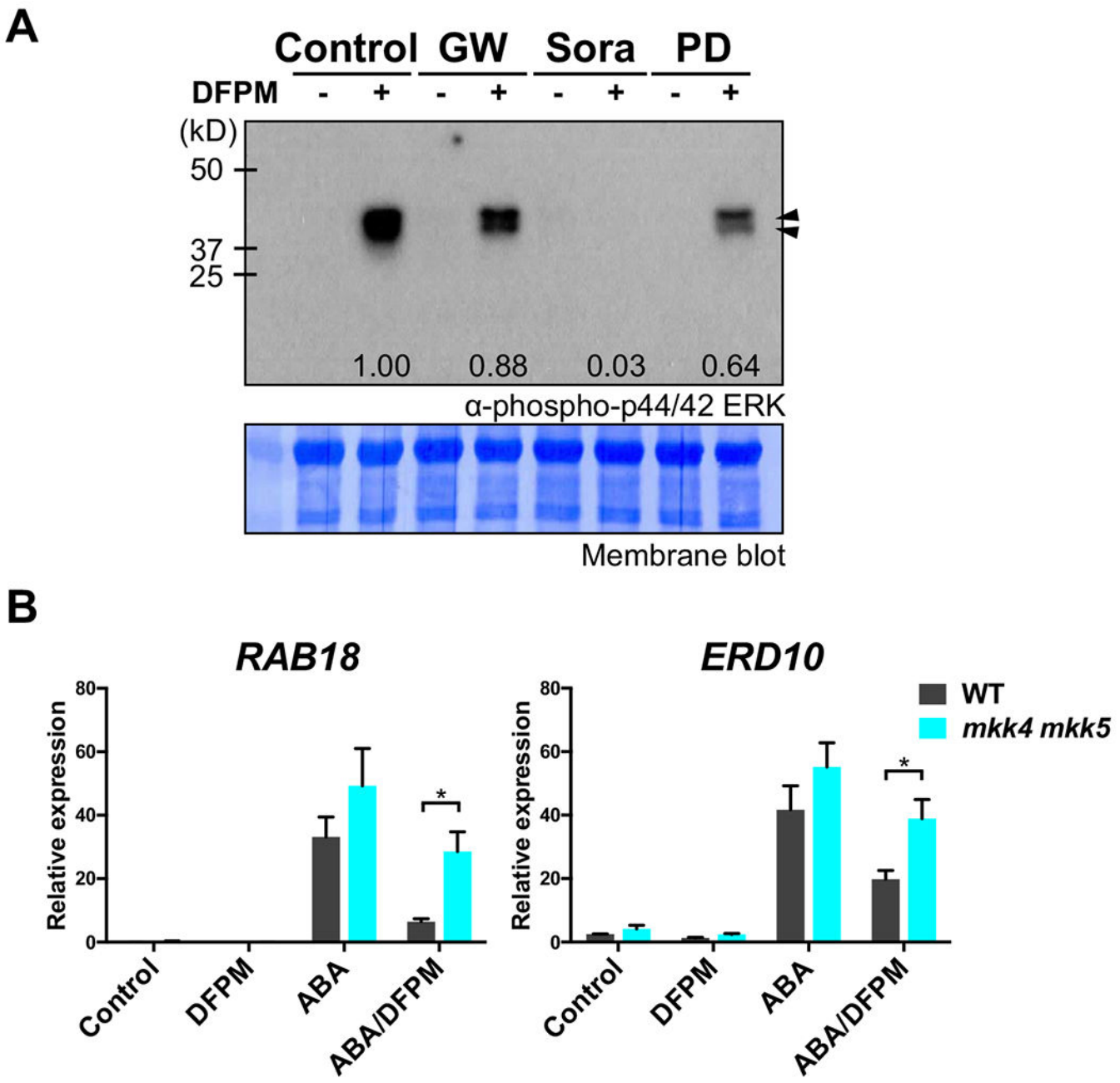

Figure 8. Involvement of MAP kinase cascades in DFPM signaling.

(A) Sorafenib, an inhibitor for Raf-type MAPKKKs suppressed DFPM-mediated activation of MAP kinases (arrowheads), while other MAPK cascade inhibitors GW5074 and PD098059 did not exhibit a clear inhibition. Wild-type Col-0 plants were treated with 30 μM DFPM or solvent control in the presence of 10 μM of inhibitors for MAPKKs and MAPKKKs, GW5074 (GW), Sorafenib (Sora) or PD098059 (PD). Phosphorylated MAPKs were detected by Western blotting using anti-phospho-p44/42 MAPK (Erk1/2) (Thr202/Tyr204) antibody. A representative result from two biological repeats is shown. The intensity

of phosphorylated MPK3 and MPK6 bands was quantified and is presented as ratios to the DFPM control without inhibitor treatment.

(B) DFPM-mediated inhibition of ABA marker gene expression was less pronounced in *mkk4 mkk5* mutant plants when compared to Col-0 wild type plants (WT). Plants were pre-treated with 30 μM DFPM or solvent control for 1 hour and then incubated in 10 μM ABA or solvent control for additional 5 hours. Expression levels were normalized with the housekeeping gene *PDF2*. Averages of 4 biological replicates are shown. Error bars = SEM. Asterisks represent $P < 0.05$ based on two-way ANOVA and Sidak's test.